

1 **Reply to Comments from Reviewer #1**

2 We thank the editor and reviewers' comments which help us to improve the manuscript.
3 We have carefully revised our manuscript following the reviewers' comments. A point-to-point
4 response is given below. The reviewers' comments are in black and our replies are in blue.

5

6 **To reviewer**

7 ***Comment 1:***

8 The authors mention that mercury species were measured but only GEM data are presented
9 and their trend calculated. What was the contribution of GOM and PBM? Could they contribute
10 to the trend? This is important to discuss because the regional atmospheric Hg emissions in
11 Section 2.5 are probably not only those of GEM but of total mercury. What was the seasonal
12 variation of GOM and PBM? Could it provide some additional evidence for the reasons of
13 GEM seasonal variation?

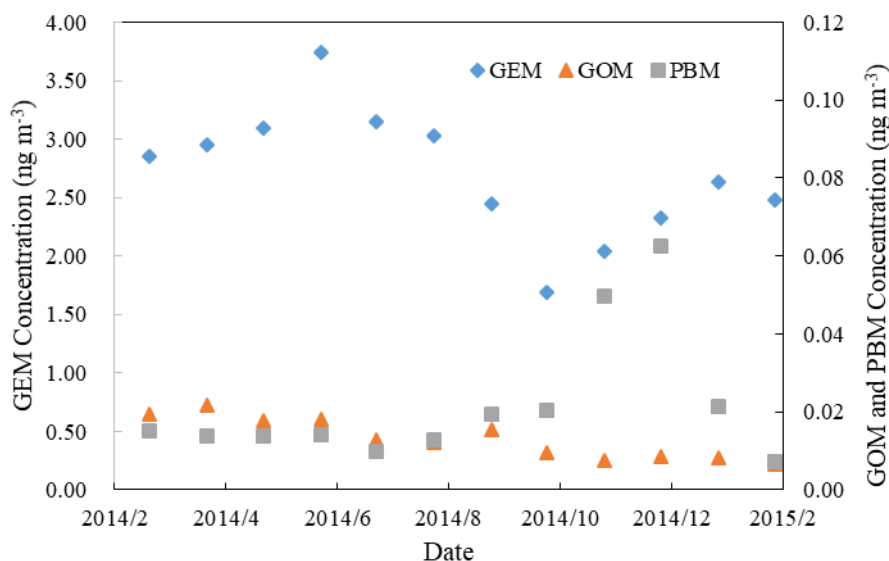
14 ***Response:***

15 The average GOM and PBM concentrations during the studied period were $14.81 \pm 13.21 \text{ pg}$
16 m^{-3} and $20.10 \pm 34.02 \text{ pg m}^{-3}$, which accounted for 0.68% and 0.92% in total Hg, respectively.
17 Therefore, the contribution of GOM and PBM to total Hg trend was supposed to be negligible.
18 The downward trend of atmospheric Hg was dominated by the GEM concentration.

19 It is true that anthropogenic Hg emission inventories included GEM, GOM and PBM
20 emissions. However, the residence time of GOM and PBM is shorter than that of GEM,
21 generally several days to a few weeks for GOM and PBM and 0.5 – 2 year for GEM (Schroeder
22 and Munthe, 1998). In addition, the concentrations of GOM and PBM were affected by
23 emissions, weather condition and depositon processes simultaneously. Therefore, the GEM
24 concentrations in the air of a background site are primarily impacted by GEM emissions. Thus,
25 the regional atmospheric Hg emissions in Section 2.5 are GEM emissions instead of total Hg
26 emissions. We have added sentences to make this point clear in Section 2.5.

27 Figure R1 showed the seasonal variation of GOM and PBM from March 2014 to February
28 2015. Considering that the concentrations of GOM and PBM were affected by emissions,
29 weather condition and depositon processes simultaneously, we need more researches to

30 determine the dominant impact factors. So it is hard to get some additional evidence for the
31 reason of GEM seasonal variation from the seasonal variation of GOM and PBM.



32 **Figure R1.** Monthly variation of GEM, GOM and PBM at Chongming from March 2014 to
33 February 2015

34

35 The calculation process of GEM emissions is revised as below.

36 “Regional atmospheric GEM emissions by month are calculated by using both the
37 technology-based emission factor methods and transformed normal distribution function
38 method. Detailed introduction of these two methods and the speciation profile of the emitted
39 Hg for each sector are described in our previous study (Wu et al., 2016).”

40 **See the revised manuscript, line 203-206**

41

42 **Comment 2 :**

43 Section 3.1: Averages and their standard deviations should always be stated with the number
44 of measurements because only then statistical tests for significance of differences can be made.
45 In line 194 the authors claim that GEM concentrations in 2014 were significantly higher than...
46 - at which significance level? Line 199: the annual decrease rate should be given with its
47 uncertainty and number of months.

48 **Response:**

49 Both the standard deviation and the number of measurements have been added in the text for

50 statistical tests of significance of differences.

51 The GEM concentrations in 2014 were significantly higher than the background
52 concentration of Northern Hemisphere at the significance level with p value less than 0.01.

53 “The GEM concentrations in 2014 were higher (t test, $p < 0.01$) than the Northern Hemisphere
54 back-ground concentration (about 1.5 ng m^{-3}) (Sprovieri et al., 2010) and those measured in
55 other remote and rural locations in China (Zhang H et al., 2015; Fu et al., 2008a; Fu et al.,
56 2009).”

57 **See revised manuscript, line 228 - 231.**

58

59 The annual decrease rate has been given with its uncertainty and the number of months. In
60 addition, the number of valid data to calculate the monthly average is listed in Table S3.

61 “During this period, monthly GEM concentrations showed a significant decrease with a rate of
62 $-0.60 \pm 0.08 \text{ ng m}^{-3} \text{ yr}^{-1}$ ($R^2 = 0.64$, $p < 0.01$ significance level, $n = 32$) (Figure 2a).”

63 **See revised manuscript, line 233 - 234.**

64

65 **Table S3.** The number of valid data during sampling period

Year	Jan	Feb	Mar	Apr	May	Jun	Jul	Aug	Sep	Oct	Nov	Dec
2014			5914	6125	6493	5568	4634	6255	6491	7106	7578	5564
2015	5227	4532	5216	3392	4072	4797	7591	6538	3434	2223	4363	8833
2016			1370	8293	7476	5884	5424	5641	3561	4544	6292	4589

66 **See revised manuscript, supporting information Table S3.**

67

68 **Comment 3:**

69 Figure 3: It is not clear how the points in Figure 3 were calculated? Were the data detrended
70 before the averaging? In view of the strong downward trend they should be. What is the
71 standard deviation or standard error of the monthly means – please show them as vertical bars
72 in Fig. 3. Are the differences between the months statistically significant? This is a precondition
73 for the discussion of the seasonal variation.

74 **Response:**

75 The GEM concentrations in the same month but different years were averaged to get monthly

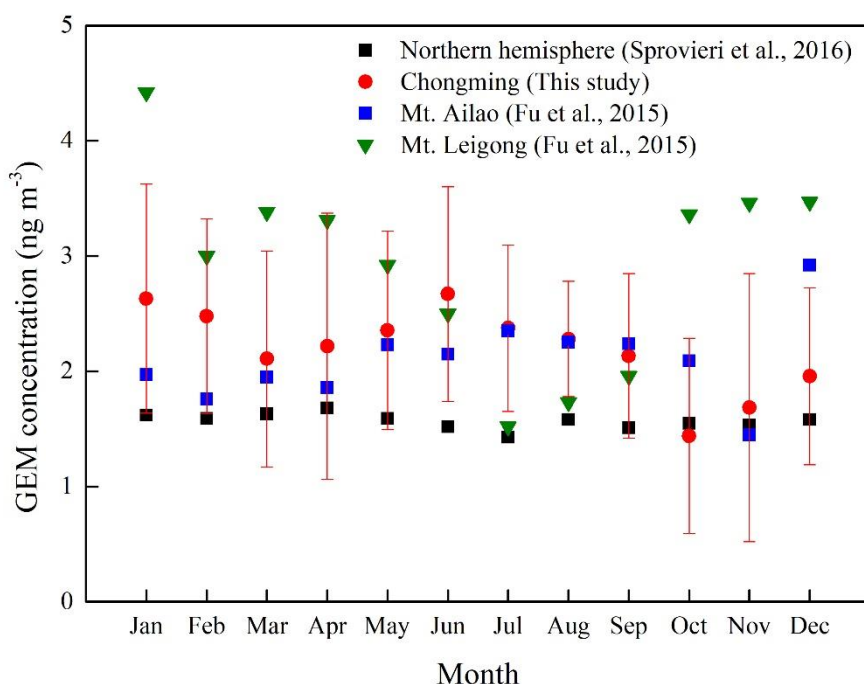
76 average during sampling period. The monthly GEM concentrations were detrended before the
77 average (Figure 2). The standard deviations of the monthly means have been added.

78

79 “According to the decomposition result (Figure 2c), we observed strong seasonal cycle at
80 Chongming. The GEM concentrations were highest in July and lowest in September, so GEM
81 concentrations in the same month from different years were averaged to understand the
82 detrended seasonal circle (Figure 3). The error bars in the Figure 3 meant the standard deviation
83 of the monthly average.”

84 See revised manuscript, line 270 –274.

85



86 **Figure 3.** Monthly variations of GEM concentration at remote sites in China

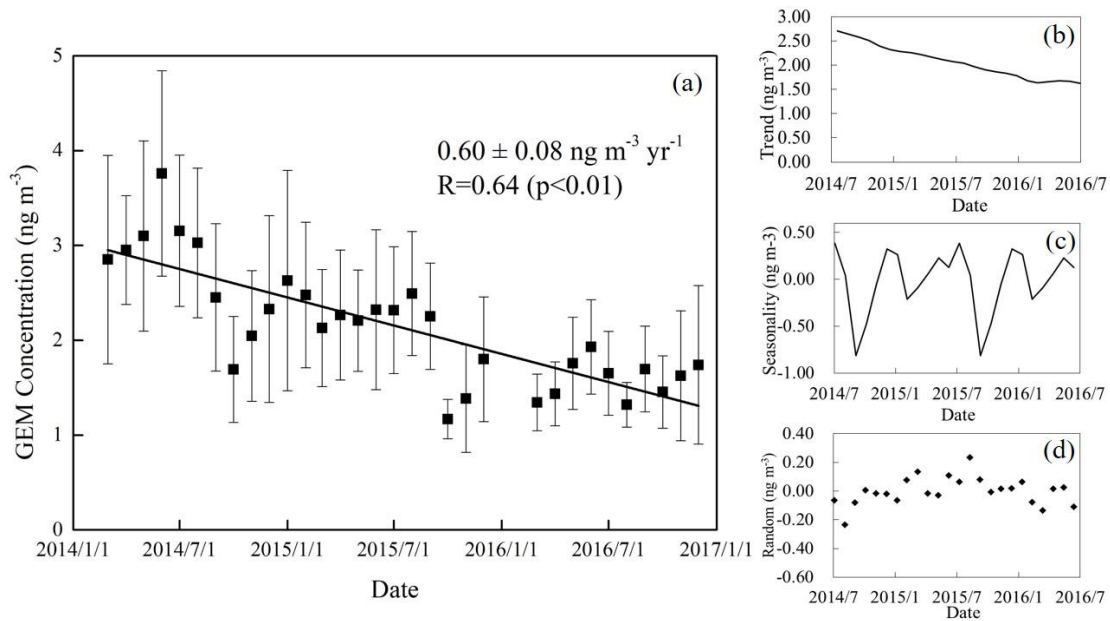
87 See revised manuscript at Figure 3.

88

89 The difference between month are statistically significant (F test, $p < 0.001$). In addition, the
90 observed GEM concentration signal was decomposed (signal = trend + seasonal + random,
91 example here: <https://anomaly.io/seasonal-trend-decomposition-in-r/>). By using this method,
92 we also observed very strong detrended seasonal cycle where GEM peak was observed in July

93 and the GEM trough was in September.

94



95

96 **Figure 2.** Monthly average GEM concentrations during the studied period (a) observed monthly
97 GEM concentrations (b) GEM trend after decomposition (c) GEM seasonality after
98 decomposition (d) GEM random after decomposition

99 Note: The observed concentrations during July 2015-April 2016 were TGM concentrations indeed
100 due to the problems of Tekran 1130/1135. However, the GOM concentrations at Chongming island
101 accounted for less than 1% of TGM. Thus, the GEM concentrations were approximated to TGM
102 concentrations during July 2015-April 2016.

103

104 **Comment 4:**

105 4.1 Figure 4 and its capture: This figure needs substantial revision to illustrate the point the
106 authors make and to make it understandable for the readers. Negative emissions are deposition
107 fluxes and should be named as such. Thus “natural emissions” in spring, autumn and winter are
108 in fact deposition fluxes. Net fluxes are needed to illustrate the point made by the authors but
109 they are not shown. The capture should also state that it is about the emissions and depositions
110 in the YRD region?

111 **Response:**

112 The natural emissions in the manuscript are defined as the followings.

113 Nature emissions=bi-directional Hg flux × studied period × studied area.

114 Therefore, emissions and flux are different concepts in this study. We use “natural emissions”
115 instead of “natural flux” to correspond to “anthropogenic emissions”. It should be pointed out
116 that the natural emission is a concept of net natural emission, which reflected a net effect of
117 two competing processes (Zhang, 2009): total natural Hg emissions and total Hg deposition.
118 When the value is positive, it means the net effect is Hg emissions to air. Otherwise, Hg
119 deposits. We have made this concept clear in both text and Figure 4.

120

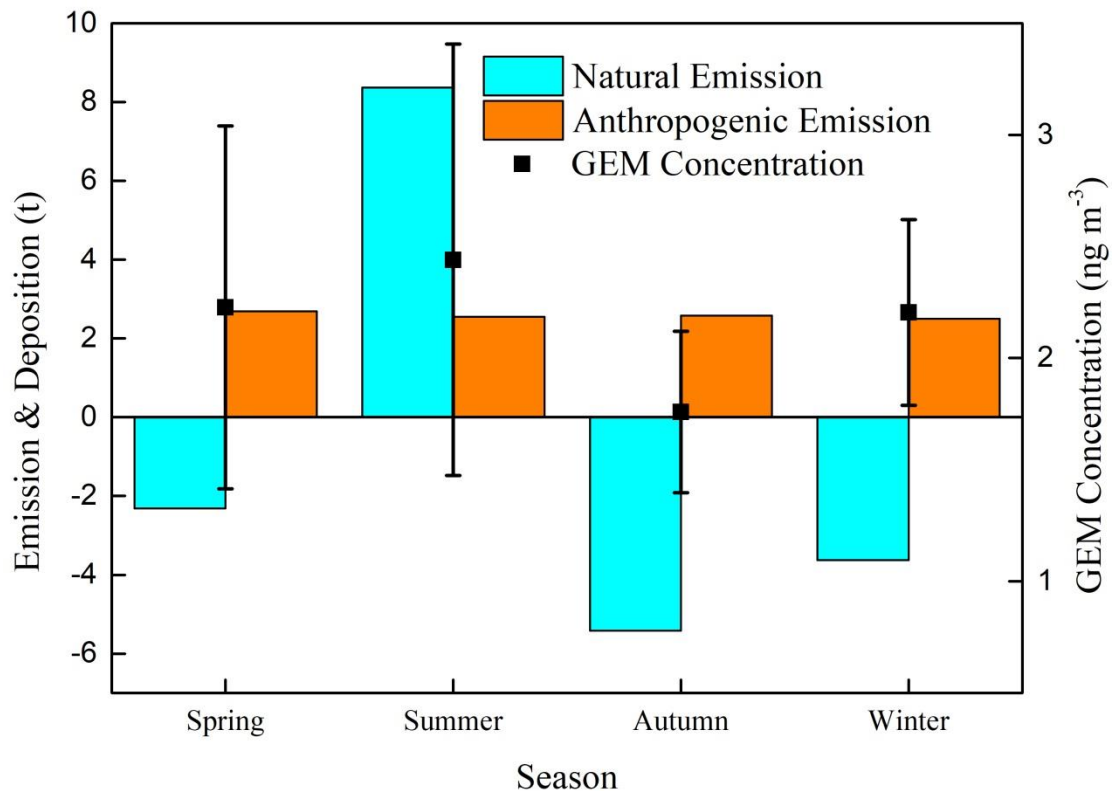
121 “The GEM emissions from natural sources E_N are calculated as followings.

$$122 \quad E_N = \sum_i F_i \times A_i \times t \quad (6)$$

123 Where F_i is a bi-directional Hg flux of canopy i , $\text{ng km}^{-2} \text{yr}^{-1}$; A is the studied area, km^2 ; t is
124 the studied year, yr. The bi-directional Hg flux was obtained from the study of Wang et al. (2016)
125 directly. It should be pointed out that the natural emission is a concept of net emission in this
126 manuscript, which reflected a net effect of two competing processes (Zhang, 2009): total Hg
127 natural emissions and total Hg deposition. The total natural emissions included primary natural
128 release and re-emission of legacy Hg stored in the terrestrial and water surface (Wang et al.,
129 2016). When the value is positive, it means the net effect is Hg emissions to air. Otherwise, Hg
130 deposited.”

131 **See revised manuscript at line 216 – line 224.**

132



133

134 **Figure 4.** Seasonal cycle of GEM concentrations and natural emissions during 2014-2016. The
 135 error bars represent the standard deviation of seasonal average. Positive values of natural
 136 emissions represent Hg emitted to air. Otherwise, Hg deposited.

137 **See the revised manuscript Figure 4.**

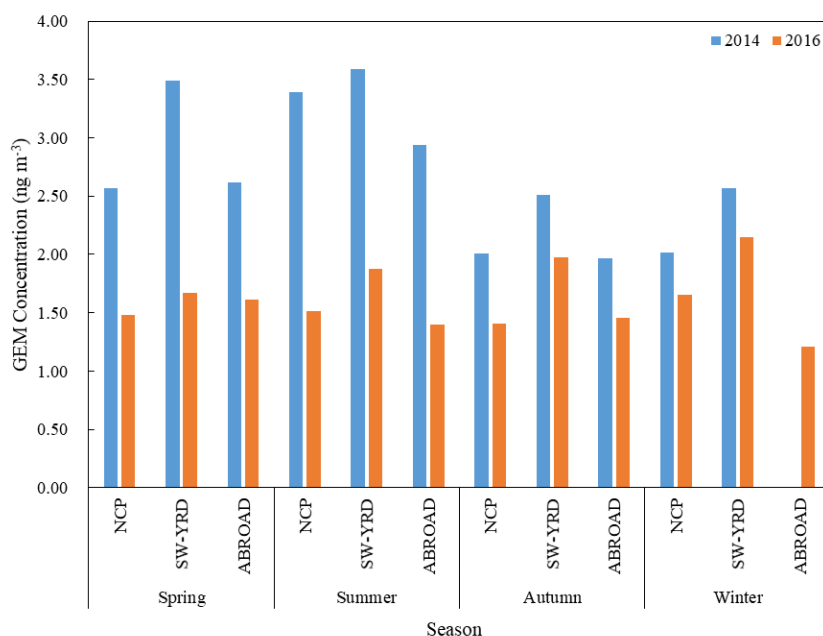
138

139 4.2 This will rise a problem: trajectory analysis in section 3.4 shows large influence of transport
 140 from the NW provinces of China outside of the YRD region. How does this transport influence
 141 the seasonal variation?

142 **Response:**

143 Trajectory outside of the YRD region showed similar seasonal variation as those passes through
 144 YRD region. The original definition of “NW” “SW” and “EAST” did not clearly distinguish
 145 the pathway of trajectory. Thus, the original “NW” actually contains the Jiangsu province of
 146 YRD region. In our revised manuscript, the trajectories were grouped into 3 clusters: NCP, SW-
 147 YRD and ABROAD. The NCP mainly passed through north China plain and around regions
 148 but not via the YRD regions; the SW-YRD passed through the YRD regions before arriving to
 149 Chongming island; the ABROAD mainly originated from the East China Seas, South Korea,

150 Japan and Northeast Asia continent, and then arrived to our monitoring sites directly without
 151 passing the mainland China. From Figure S3, we can see that the NCP cluster and
 152 ABROAD cluster showed similar seasonal variation as cluster SW-YRD. High GEM
 153 concentrations were observed in summer.



154 **Figure S3.** The seasonality of GEM concentration in the NCP, SW-YRD and ABORD region
 155 (No trajectory transport though ABROAD in winter of 2014)

156 We also revised the manuscript as below.

157 “Transport also overall enhanced the observed seasonal variation of GEM concentrations at
 158 Chongming Island. According to the statistics of backward trajectories in section 3.4, the GEM
 159 concentrations in the air mass which did not pass via the YRD regions also showed high GEM
 160 concentration in warm season in 2014 (Figure S3).”

161 **See the revised manuscript at line 309 - 312**

162

163 **Comment 5:**

164 Line 243-245: “The annual emissions from both natural source and anthropogenic source...
 165 was 0.75 and 10.3 t, respectively” – the reader may think that natural emissions make less than
 166 10% of the anthropogenic ones and cannot thus be responsible for the seasonal variation. One
 167 has to look in Fig. 4 to find out that the “natural emissions” are a sum of natural emissions in
 168 one season and “natural” deposition fluxes in three seasons. That provokes a question: how is

169 anthropogenically emitted mercury removed from the atmosphere if there are only “natural”
170 deposition fluxes? Please use the correct terminology and separate the natural and
171 anthropogenic emissions from the deposition fluxes of both.

172 **Response:**

173 Sorry for the misunderstanding. To avoid confusion, we deleted the sentence of “The annual
174 emissions from both natural source and anthropogenic source... was 0.75 and 10.3 t,
175 respectively” in the revised manuscript. The impact of anthropogenic emissions and natural
176 emissions were discussed separately. The anthropogenic emissions were in the range of 2.5 –
177 2.7 t while natural emissions varied from -5.4 – 8.4 t in different season. Thus, one important
178 conclusion of our study is that the seasonal GEM cycle was dominated by the natural
179 emissions.

180 “Source emission is one significant factor on GEM concentrations in the air. The GEM
181 concentrations at a remote site are generally regarded under the impact of regional emissions.
182 Therefore, the emissions in the YRD regions (Anhui, Zhejiang, Jiangsu, and Shanghai) were
183 calculated. However, the anthropogenic emissions were in the range of 2.5-2.7 t, which is
184 almost unchanged. Compared to the anthropogenic emissions, we observed almost
185 synchronized trends between natural emissions and air Hg concentrations in Figure 4.”

186 **See the revised manuscript at line 291 - 306**

187

188 It is difficult to distinguish whether the deposited Hg is from natural sources or anthropogenic
189 sources. Therefore, the bi-directional Hg flux scheme contained total Hg deposition flux (both
190 so called “natural” and “anthropogenic” deposition fluxes) (Zhang et al., 2009). And the natural
191 Hg emissions in this study have considered the removal of anthropogenic Hg emissions. We
192 have clearly defined the concept of “natural emissions” in this study. The natural emission is a
193 concept of net natural emission, which reflected a net effect of total natural Hg emissions and
194 total Hg deposition amount. Therefore, the data of natural emissions in the four seasons contains
195 both emissions and deposition. The positive value in summer means that net effect is Hg
196 emissions to air. In other three seasons, Hg deposited. Detailed revision is described as follows.

197 “The GEM emissions from natural sources E_N are calculated as followings.

198

$$E_N = \sum_i F_i \times A_i \times t$$

199 where F_i is a bi-directional Hg flux of canopy i , $\text{ng km}^{-2} \text{ yr}^{-1}$; A is the studied area, km^2 ; t is the
200 studied year, yr. The bi-directional Hg flux was obtained from the study of Wang et al. (2016)
201 directly. It should be pointed out that the natural emission is a concept of net emission in this
202 manuscript, which reflected a net effect of two competing processes (Zhang, 2009): total Hg
203 natural emissions and total Hg deposition. The total natural emissions included primary natural
204 release and re-emission of legacy Hg stored in the terrestrial and water surface (Wang et al.,
205 2016). When the value of E_N is positive, it means the net effect is Hg emissions to air. Otherwise,
206 Hg deposited.”

207 **See the revised manuscript at line 215 - 223**

208

209 **Comment 6:**

210 The results of PCA analysis and Table 2: The authors attribute the factor 2 to “exchange of
211 PBL with free troposphere” but do not explain why. Last row in the table 2 called “variance
212 explain” lists for 2016 exchange of PBL with the free troposphere 75.735 which together with
213 50.625 for “combustion” makes more than 100. As such the units of “variance explain” cannot
214 be percent. What are the numbers in this row and does it make sense to present them with three
215 valid numbers after decimal point?

216 **Response:**

217 We have added explanation as follows.

218 “Considering the low loading of CO and high loading of O₃, the factor 2 can be viewed as a
219 sign of the transport of air mass from stratosphere (Fishman and Seiler, 1983; Jaffe, 2010). The
220 air mass from stratosphere will increase the O₃ concentration. O₃ react with NO, which makes
221 a negative correlation with NO. However, the low loading on GEM of factor 2 indicated that
222 Factor 2 had no relationship with GEM concentrations at Chongming from the aspect of whole
223 year data.”

224 **See the revised manuscript at line 345 - 350**

225

226 Sorry for the typo. We have corrected this in Table 1. The variance explain showed the

227 contribution ratio of factor 1 and factor 2 in the total variance. We have revised the data to two
 228 valid numbers after decimal point.

229 **Table 1.** PCA component loading of GEM and other air pollutants

Air pollutants	2014		Air pollutants	2016	
	Factor 1	Factor 2		Factor 1	Factor 2
SO ₂	0.76	0.14	SO ₂	0.82	-0.09
NO _x	0.76	-0.20	NO _x	0.70	-0.52
O ₃	-0.11	0.98	O ₃	-0.41	0.97
PM _{2.5}	0.85	0.05	PM _{2.5}	0.88	0.05
GEM	0.66	0.02	GEM	0.78	-0.19
CO	0.79	0.12			
Component	Combustion	Transport of air mass from stratosphere	Component	Combustion	Transport of air mass from stratosphere
Variance explain (%)	49.36	17.53	Variance explain (%)	50.63	25.10

230 Note: Text in bold phase were regarded as high loading (factor loading>0.40 or <-0.40)

231

232 **Comment 7:**

233 Table 3: The numbers are probably annual emissions but the capture does not say it. The year
 234 of the emissions is not given. I wonder about the “other SO₂ sources” which are substantially
 235 larger than all coal, oil, and biomass burning taken together. If it is not an error, what are the
 236 “other SO₂ sources”?

237 **Response :**

238 Thank for the comments. It is the emission in 2014. The emission for “other SO₂ sources” is
 239 a typo and we have revised this. The other sectors contain municipal solid incineration, copper
 240 smelting, aluminum production, gold production, other coal combustion, stationary oil
 241 combustion, and cremation. Table 2 has been revised as follows.

242 **Table 2.** Emissions of the main air pollutants in YRD region in 2014

Sectors	Annual emissions			
	SO ₂ (kt)	NO _x (kt)	PM _{2.5} (kt)	GEM (t)
Coal-fired power plants	918.31	991.62	118.42	14.00
Coal-fired industrial boilers	311.03	271.94	79.91	9.80
Residential coal combustion	68.48	42.11	163.93	0.40
Cement clinker production	207.48	371.13	208.02	4.70
Iron and steel production	480.97	142.80	169.84	2.30
Mobile oil combustion	38.43	1786.74	98.00	1.90

Other sectors	348.83	316.28	382.48	2.50
---------------	--------	--------	--------	------

243 “The studied emission sectors included coal-fired power plants, coal-fired industrial boilers,
 244 residential coal-combustion, cement clinker production, iron and steel production, and other
 245 small emission sectors (eg., zinc smelting, lead smelting, municipal solid incineration, copper
 246 smelting, aluminum production, gold production, other coal combustion, stationary oil
 247 combustion, and cremation).”

248 **See the revised manuscript at line 209 - 212**

249

250 **Comment 8:**

251 Chapter 3.4 misses a major point: Table 3 of SO₂, NO_x, PM_{2.5}, and GEM emissions is only
 252 for one undefined year and only for the YRD region. Table 4 and Figure 6 show a dominant
 253 influence of transport from NW of China which is mostly outside of the YRD region. To
 254 illustrate convincingly the major conclusion of the paper one would need a table with the
 255 inventories for NW and SW (perhaps separately) and for 2014 and 2016.

256 **Response :**

257 According to our response to comment 4, we have adjusted the cluster. Based on the adjusted
 258 cluster, we added the emissions of SO₂, NO_x and PM_{2.5} in both 2014 and 2016 to illustrate the
 259 change of emission inventory in NCP and SW-YRD region (Table S5). According to the table,
 260 we observed obvious emission decline of the above pollutants.

261 **Table S5.** Emission inventories of the main pollutants from the studied regions in 2014 and
 262 2016

Air pollutants	2014		2016		Decline proportion	
	NCP	SW-YRD	NCP	SW-YRD	NCP	SW-YRD
PM _{2.5} (kt)	2019	1209	1849	1109	-8%	-8%
NO _x (kt)	5697	4022	5424	3855	-5%	-4%
SO ₂ (kt)	3780	1993	3450	1780	-9%	-11%
GEM (t)	118	72	103	67	-13%	-7%

263 Note: According to the contribution of trajectory, the dominant provinces in the NCP region
 264 included Beijing, Tianjin, Hebei, Shandong and Liaoning province. The SW-YRD mainly
 265 contained Shanghai, Zhejiang, Jiangsu, Jiangxi and Anhui province.

266 **See the revised manuscript at line 377 - 379**

267

268 ***Comment 9:***

269 Table 1: The paper is about regional trend and I wonder why it is necessary to discuss global
270 background trends in such detail. Also because the reasons of downward trend of mercury at
271 many background stations of the world at the time of increasing global emissions is still not
272 well understood (compare Horowitz et al., EST 48, 10242-10250, 2014, with Soerensen et al.,
273 GRL, 39, L21810, doi:10.1029/2012GL053736, 2012).

274 ***Response :***

275 We agree with your valuable comment. Our paper is about regional trend, so we have
276 curtailed the discussion and move the original Table 1 to supporting information (Table S4) so
277 as to focus on our topic.

278

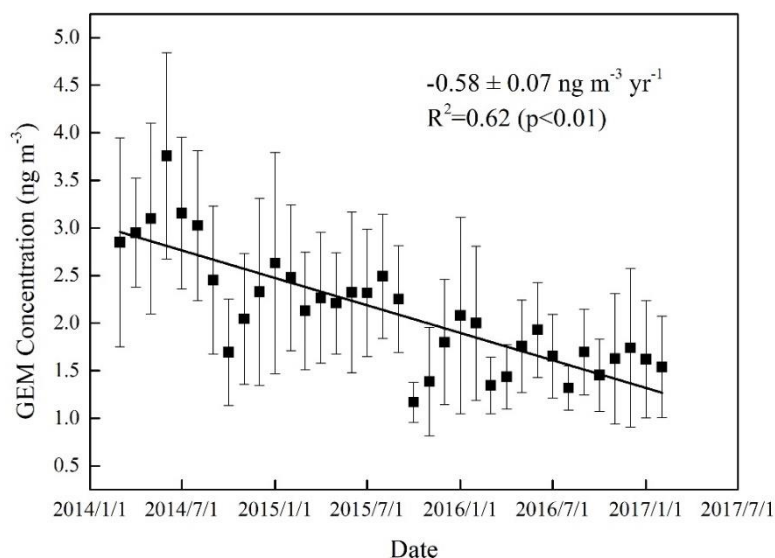
279 ***Comment 10:***

280 Figure S1: Here the least square fit of 4 points provides R² of 0.487 for January and 0.613 for
281 February for which the authors claim $p < 0.01$ in both cases. This is surely incorrect because 4
282 points result statistically in only 2 degrees of freedom. Please explain.

283 ***Response :***

284 The purpose of original Figure S1 is to obtain the fitting curve so as to calculate the Hg
285 concentrations in the January and February of 2016. But it did not work actually because the
286 points are not enough. Therefore, we deleted the original Figure S1. Instead, the average value
287 of the GEM concentrations in January of 2015 and 2017 were used to represent the GEM
288 observation in January of 2016. The same method is used to simulate the GEM observation in
289 February of 2016.

290 The Figure S1 was revised as below.



291 **Figure S1.** The trend of monthly average GEM concentration from March 2014 to February
292 2017. The monthly average of GEM in January of 2016 is simulated as the average value that
293 in the January of 2015 and 2017. The same method is used for the data in February of 2016.

294

295 **Comment 11:**

296 Figure S2: The downward annual rate should be given with its standard error.

297 **Response:**

298 The downward annual rate was given with its standard error as follows. See the Figure S1 in
299 the response of comment 10.

300

301 **Comment 12:**

302 Line 51: “Both GOM and PBM are more soluble.” than what? PBM is not necessarily more
303 soluble than GEM but it is scavenged by wet deposition. Low solubility of GEM need to be
304 mentioned before this statement.

305 **Response :**

306 The statement has been revised as follows.

307 “GOM is more soluble than GEM, and PBM can be quickly scavenged by both dry and wet
308 deposition. Therefore, the residence time of both GOM and PBM is shorter than that of GEM,
309 generally several days to a few weeks for GOM and 0.5 – 2 year for GEM (Schroeder and

310 Munthe, 1998). ”

311 **See the revised manuscript at line 52 - 55.**

312

313 ***Comment 13:***

314 Lines 71/72: ...have been estimated to decrease...

315 ***Response :***

316 We have revised the manuscript as follow.

317 “However, recently atmospheric Hg emissions in China have been estimated to decrease since

318 2012 (Wu et al., 2016).”

319 **See the revised manuscript at line 82**

320

321 ***Comment 14:***

322 Line 86: ...is located...

323 ***Response:***

324 We have revised the manuscript as suggested.

325 “As China’s third largest island, Chongming Island is located in the east of Yangtze River Delta

326 region with a typical subtropical monsoon climate.”

327 **See the revised manuscript at line 97**

328

329 ***Comment 15:***

330 Lines 102/103: ... the error between gold trap A and gold trap B was limited to...? Probably

331 the difference instead of error was limited. What happens if the difference is more than the

332 limit?

333 ***Response:***

334 We have replaced the error with differences. If the difference is more than the limit, it means

335 that the gold traps are passivizing and we need to replace the old gold trap A and gold trap B.

336

337 ***Comment 16:***

338 Lines 171/172: “uncertainties” would be better than “errors”

339 **Response:**

340 We have revised the manuscript as suggested.

341

342 **Comment 17:**

343 Line 199: Please state the decrease rate with its standard error.

344 **Response**

345 We have revised the manuscript as suggested.

346

347 **Comment 18:**

348 Lines 207-209: A reference to Martin et al (2017) is not correct because the paper does not
349 contain annual averages and the authors of this paper do not mention a gap in the measurements
350 between 2004 and 2007. The correct reference would be: annual average GEM concentration
351 decreased from 1.29 ng m⁻³ in 1996 to 1.19 ng m⁻³ in 2004 (Slemr et al., GRL 35, L11807,
352 doi:10.1029/2008GL033741, 2008) and were increasing from 0.93 ng m⁻³ in 2007 (Slemr et
353 al., ACP 15, 3125-3133, 2015) until 2016 (Martin et al, 2017).

354 **Response:**

355 We have revised the manuscript as suggested.

356 “In South Africa, annual average GEM concentration at Cape Point decreased from 1.29 ng
357 m⁻³ in 1996 to 1.19 ng m⁻³ in 2004 (Slemr et al., 2008) and were increasing from 0.93 ng m⁻³
358 in 2007 (Slemr et al., 2015) until 2016 (Martin et al, 2017).”

359 **See the manuscript at line 257– 259**

360

361 **References:**

362 Fishman J, Seiler W. Correlative Nature of Ozone and Carbon Monoxide in the Troposphere:
363 Implications for the Tropospheric Ozone Budget. Journal of Geophysical Research, 88(C6), 1983.

364 Jaffe, D.: Relationship between surface and free tropospheric ozone in the western U.S.,
365 Environmental Science & Technology, 45, 432-438, 10.1021/es1028102, 2010.

366 Li S, Gao W, Wang S X, Zhang L, Li Z J, Wang L, Hao J M. Characteristics of Speciated
367 Atmospheric Mercury in Chongming Island, Shanghai. Environmental Science 2016, 37(9): 3290 -

368 3299.

369 Pirrone N, Cinnirella S, Feng X, Finkelman R B, Friedli H R, Leaner J, Mason R, Mukherjee A B,
370 Stracher G B, Streets D G, Telmer K. Global Mercury Emissions to the Atmosphere from
371 Anthropogenic and Natural Sources. *Atmospheric Chemistry and Physics*, 2010, 10(13): 5951-5964.
372 Slemr F, Angot H, Dommergue A, Magand O, Barret M, Weigelt A, Ebinghaus R, Brunke E G,
373 Pfaffhuber K A, Edwards G, Howard D, Powell J, Keywood M, Wang F. Comparison of Mercury
374 Concentrations Measured at Several Sites in the Southern Hemisphere. *Atmospheric Chemistry and*
375 *Physics*, 2015, 15(6): 3125-3133.

376 Sprovieri F, Pirrone N, Bencardino M, amp, apos, Amore F, Carbone F, Cinnirella S, Mannarino V,
377 Landis M, Ebinghaus R, Weigelt A, Brunke E-G, Labuschagne C, Martin L, Munthe J, W ängberg I,
378 Artaxo P, Morais F, Barbosa H d M J, Brito J, Cairns W, Barbante C, Di éguez M d C, Garcia P E,
379 Dommergue A, Angot H, Magand O, Skov H, Horvat M, Kotnik J, Read K A, Neves L M, Gawlik
380 B M, Sena F, Mashyanov N, Obolkin V, Wip D, Feng X B, Zhang H, Fu X, Ramachandran R, Cossa
381 D, Knoery J, Maruszczak N, Nerentorp M, Norstrom C. Atmospheric Mercury Concentrations
382 Observed at Ground-Based Monitoring Sites Globally Distributed in the Framework of the Gmos
383 Network. *Atmospheric Chemistry and Physics*, 2016, 16(18): 11915-11935.

384 Wang X, Lin C J, Yuan W, Sommar J, Zhu W, Feng X. Emission-Dominated Gas Exchange of
385 Elemental Mercury Vapor over Natural Surfaces in China. *Atmospheric Chemistry and Physics*,
386 2016, 16(17): 11125-11143.

387 Wang X, Lin C J, Feng X. Sensitivity Analysis of an Updated Bidirectional Air–Surface Exchange
388 Model for Elemental Mercury Vapor. *Atmospheric Chemistry and Physics*, 2014, 14(12): 6273-6287.

389 Zhang L, Wang L, Wang S, Dou H, Li J, Li S, Hao J. Characteristics and Sources of Speciated
390 Atmospheric Mercury at a Coastal Site in the East China Sea Region. *Aerosol and Air Quality*
391 *Research*, 2017, 17(12): 2913-2923.

392 Zhang, L. M., Wright, L. P., and Blanchard, P.: A review of current knowledge concerning dry
393 deposition of atmospheric mercury, *Atmos. Environ.*, 43, 5853-5864, 2009.

394 Zhang Y, Jacob D J, Horowitz H M, Chen L, Amos H M, Krabbenhoft D P, Slemr F, St Louis V L,
395 Sunderland E M. Observed Decrease in Atmospheric Mercury Explained by Global Decline in
396 Anthropogenic Emissions. *Proceedings of the National Academy of Sciences of the United States*
397 *of America*, 2016, 113(3): 526.

398 **Reply to Comments from Reviewer #2**

399 We thank the editor and reviewers' comments which help us improve the manuscript. We
400 have carefully revised our manuscript following the reviewers' comments. A point-to-point
401 response is given below. The reviewers' comments are in black and our replies are in blue.

402 **To Reviewer**

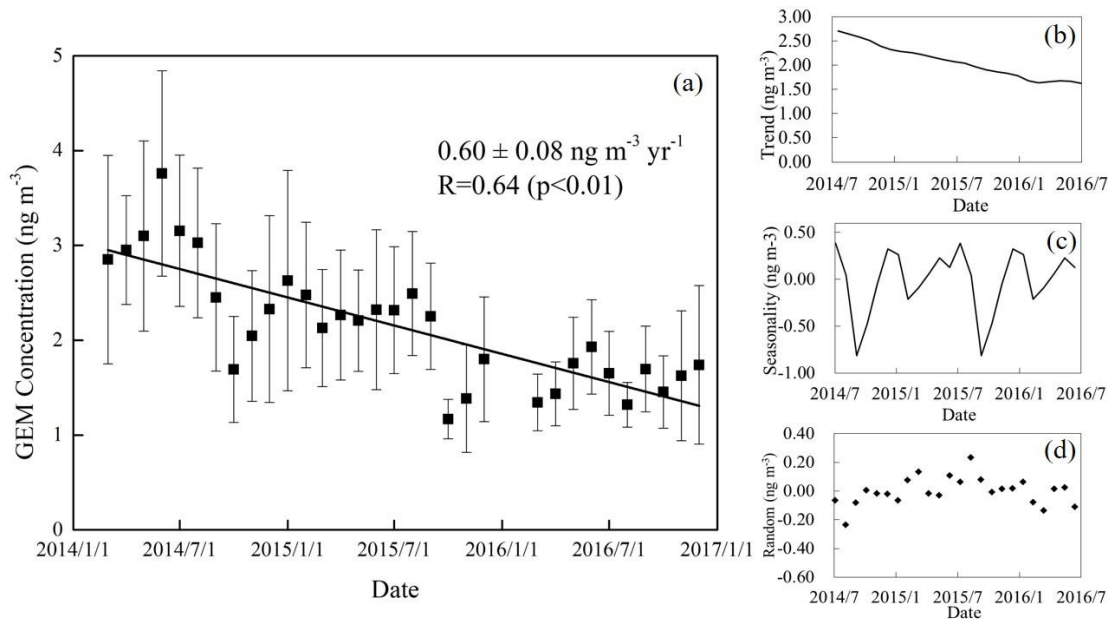
403 ***Major Comment:***

404 I really think you should perform a trend decomposition of the signal (signal = seasonal +
405 trend + random, example here: <https://anomaly.io/seasonal-trend-decomposition-in-r/>). There
406 is a very strong seasonal cycle and you conclude that "the seasonal GEM cycle was dominated
407 by the natural emissions". However, how can you explain that the seasonality is way more
408 pronounced in 2014? To me, presenting emissions inventories is not convincing enough; how
409 you can you be sure that the decreasing trend is not driven by a change in seasonality?

410 ***Response:***

411 The trend decomposition of the signal is performed in Figure 2 (signal = trend + average
412 variation + random). By using this method, the decreasing trend was shown in Figure 2b and
413 the seasonality is approximately 12 months. In each cycle, we observed very strong seasonal
414 cycle where GEM peak was observed in July and the GEM trough was in September.

415 The seasonal variation was more pronounced in 2014 can attribute to the lower wet
416 deposition and GEM oxidation. On one aspect, as a costal site, the Chongming island is
417 abundant with $\cdot\text{OH}$ radicals. The increase of O_3 concentration from the summer of 2014 to 2016
418 may contribute to a higher oxidation of GEM in 2016. On another aspect, higher wet Hg
419 deposition in summer is approximately 6.6 times of that in the winter at Chongming (Zhang et
420 al., 2010). Meanwhile, the rainfall in 2016 summer (546 mm) was higher than the rainfall in
421 2014 (426 mm). Therefore, the higher oxidation and wet deposition rate of mercury in the
422 summer of 2016 will reduce the peak of GEM concentration and then shrink the concentration
423 difference between summer and winter, which lead to a less pronounced seasonal variation in
424 2016.



425

426 **Figure 2.** Monthly average GEM concentrations during the studied period (a) observed monthly
 427 GEM concentrations (b) GEM trend after decomposition (c) GEM seasonality after
 428 decomposition (d) GEM random after decomposition

429 Note: The observed concentrations during July 2015-April 2016 were TGM concentrations
 430 indeed due to the problems of Tekran 1130/1135. However, the GOM concentrations at
 431 Chongming island accounted for less than 1% of TGM. Thus, the GEM concentrations were
 432 approximated to TGM concentrations during July 2015-April 2016.

433

434 The revised manuscript of decomposition trend is revised as below.

435 “From another aspect, the trend decomposition of the GEM concentration signal (signal =
 436 trend + seasonal + random) from March 2014 to December 2016 were performed in Figure 2
 437 (<https://anomaly.io/seasonal-trend-decomposition-in-r/>). By using this method, we also
 438 observed a pronounced trend (Figure 2b) and the random was limited in the range of -0.24 –
 439 0.24 ng m⁻³ (Figure 2d).”

440 **See the revised manuscript at line 234 - 239**

441

442 “From Figure 2, we also observed more pronounced seasonal variation in 2014, which can
 443 be attributed to the lower wet deposition and GEM oxidation. On one aspect, as a costal site,
 444 the Chongming Island is abundant with •OH. The increase of O₃ concentration from the summer

445 of 2014 to 2016 may contribute to a higher oxidation of GEM in 2016. On another aspect,
446 higher wet Hg deposition in summer is approximately 6.6 times of that in the winter at
447 Chongming (Zhang et al., 2010). Meanwhile, the rainfall in 2016 summer (546 mm) was higher
448 than the rainfall in 2014 (426 mm). Therefore, the higher oxidation and wet deposition rate of
449 Hg in the summer of 2016 will reduce the concentration difference between summer and winter,
450 which lead to a less pronounced seasonal variation in 2016. Meanwhile, the higher oxidation
451 and wet deposition in 2016 also contributed to the downward trend of GEM by reducing the
452 seasonality in spring and summer (Figure S3).”

453 **See the revised manuscript at line 314 - 324**

454

455 While SO₂, NO₂, and PM concentrations were monitored, data are not presented nor
456 discussed. Do you also observe a decreasing trend? That would be the best way to support that
457 "air pollution control policies targeting SO₂, NO₂, and PM reductions had significant co-
458 benefits on atmospheric Hg".

459 ***Response:***

460 To further verify the cause of downward trend of atmospheric Hg, we give the emission
461 inventory (Table S6) and concentrations (Table S5) of other air pollutants in the studied regions
462 in both 2014 and 2016. Both the emissions and concentrations of SO₂, NO₂, and PM showed a
463 decreasing trend, which is used to support that "air pollution control policies targeting SO₂,
464 NO₂, and PM reductions had significant co-benefits on atmospheric Hg".

465

466 “Table 3 showed the detailed data of the three classifications. From 2014 to 2016, the whole
467 China region (NCP, SW-YRD) contributed to 70% of GEM decline at Chongming Island.
468 Considering downward trend of emission inventory and atmospheric pollutant from 2014 to
469 2016 in NCP and SW-YRD region (Table S5, Table S6), the reason of downward trend can be
470 attributed to the effectiveness of existing air pollution control measures in China (SC, 2013;
471 MEP, 2014).”

472 **See the revised manuscript at line 375 – 379**

473

474 **Table S5.** The annual concentration of SO₂, NO_x, O₃ and PM_{2.5} at Chongming site, NCP, and

Year	2014			2016			Change			
Pollutants	Region	NCP	SW-YRD	Chongming	NCP	SW-YRD	Chongming	NCP	SW-YRD	Chongming
PM _{2.5} ($\mu\text{g m}^{-3}$)		71.93	53.05	25.09	60.75	44.75	23.89	-16%	-16%	-5%
SO ₂ ($\mu\text{g m}^{-3}$)		34.52	21.01	1.60	24.37	16.40	1.47	-29%	-22%	-8%
NO ₂ ($\mu\text{g m}^{-3}$)		45.07	34.34	12.62	41.55	34.40	10.84	-8%	0%	-14%
O ₃ ($\mu\text{g m}^{-3}$)		60.29	56.27	41.70	61.84	60.92	44.38	3%	8%	6%
GEM (ng m^{-3})		No data		2.68	No data		1.60	No data		-40%

476 Note: According to the contribution of trajectory, the dominant provinces in the NCP region
 477 included Beijing, Tianjin, Hebei, Shandong and Liaoning province. The SW-YRD mainly
 478 contained Shanghai, Zhejiang, Jiangsu, Jiangxi and Anhui province.

479

480 **Table S6.** Emission inventories of the main pollutants from the studied regions in 2014 and
 481 2016

Air pollutants	2014		2016		Decline proportion	
	NCP	SW-YRD	NCP	SW-YRD	NCP	SW-YRD
PM _{2.5} (kt)	2019	1209	1849	1109	-8%	-8%
NO _x (kt)	5697	4022	5424	3855	-5%	-4%
SO ₂ (kt)	3780	1993	3450	1780	-9%	-11%
GEM (t)	118	72	103	67	-13%	-7%

482 Note: According to the contribution of trajectory, the dominant provinces in the NCP region
 483 included Beijing, Tianjin, Hebei, Shandong and Liaoning province. The SW-YRD mainly
 484 contained Shanghai, Zhejiang, Jiangsu, Jiangxi and Anhui province.

485

486 Finally, I wonder why GOM and PBM data are not reported and discussed. Do you also
 487 observe a decreasing trend? You may have encountered issues with the speciation unit. If so,
 488 was the experimental setup identical in 2014 and 2016, or did you analyze GEM when the
 489 speciation unit was working vs. TGM when it wasn't? A discussion on analytical uncertainties
 490 would be much welcomed.

491 The GOM and PBM data are not reported finally due to the following reasons. First, the main
 492 purpose of this manuscript is to validate the anthropogenic Hg emissions reduction through
 493 observation data. The Chongming sit is a background site. Considering the stability of GEM in

494 the air, we choose GEM as an index to reflect the emission control effect. Second, the method
495 we developed to explain the GEM trend is not applicable for GOM and PBM. Except emissions,
496 we think the potential reactions in the air are significant factors to impact both GOM and PBM
497 concentrations. But we need more evidence to prove our assumptions. Therefore, we deleted
498 the discussion of GOM and PBM in our final manuscript.

499 We also observed decreasing trend of PBM. But the GOM kept increasing. Currently, we
500 need more study to explain this phenomenon.

501 Yes, we also encountered issues with the speciation unit. From July 5, 2015 to April 30 2016,
502 the Tekran 1130/1135 speciation unit was damaged by the rainstorm, the Tekran 2537X were
503 operated without speciation units but with PTFE filter to protect the instrument from particles
504 and sea salt. The average concentration of GOM and PBM during sampling period was 14.81
505 ± 13.21 and 20.10 ± 34.02 pg m^{-3} , respectively. The GOM fraction in TGM was less than 1%
506 at Chongming island (Li et al., 2016; Zhang et al., 2017). Therefore, the GEM concentrations
507 were approximated to TGM concentrations July 5, 2015 to April 30 2016 when the speciation
508 unit does not work, as most of other studies have done (Slemr et al., 2015; Sprovieri et al.,
509 2016). In addition, uncertainty analysis was performed to point out potential impact. The
510 revision is as follows.

511 “From July 5, 2015 to April 30 2016, the Tekran 1130/1135 speciation unit was damaged by
512 the rainstorm, the Tekran 2537X were operated without speciation units but with PTFE filter to
513 protect the instrument from particles and sea salt. Therefore, the observed concentrations during
514 July 2015-April 2016 were TGM concentrations indeed. However, the GOM concentrations at
515 Chongming Island accounted for less than 1% of TGM (TGM=GOM+GEM). Thus, the GEM
516 concentrations were approximated to TGM concentrations from July 2015 to April 2016.”

517 **See the revised manuscript at line 109 – 115**

518 “In our research, random uncertainties of individual measurement had been averaged out and
519 the systematic uncertainties need to be considered. The overall practically achievable
520 systematic uncertainty would be 10% considering that the instrument was not in ideal
521 performance (Slemr et al., 2015; Steffen et al., 2012). For example, slow deactivation of the
522 traps, contamination of the switching valves and leaks would increase the uncertainties but were
523 difficult to quantify (Slemr et al., 2015;Steffen et al., 2012). Because of the consistency of

524 instrument and the quality assurance/quality control have been paid special attention to during
525 the sampling campaign, the systematic differences of instrument did not affect the huge
526 variation between 2014 and 2016.”

527 **See the revised manuscript at line 122 – 129**

528

529 ***Comment 1:***

530 Line 26: "GEM concentrations showed a significant decrease with a rate of -0.60 ng/m³/yr".
531 According to Table 1, the rate is -0.52 ng/m³/yr.

532 ***Response:***

533 Thanks for the comments. This is a typo in the table. It is -0.60±0.08 ng m⁻³ yr⁻¹ actually. We
534 have corrected this in the revised manuscript.

535 .

536 ***Comment 2:***

537 Line 33: "It was find" should be "It was found".

538 ***Response:***

539 We have corrected in the manuscript as below.

540 “It was found that the reduction of domestic emissions was the main driver of GEM decline
541 in Chongming Island, accounting for 70% of the total decline.”

542 **See the revised manuscript at line 33 – 34**

543

544 ***Comment 3:***

545 Lines 47-48: "In the atmosphere, Hg mainly presents as GEM, accounting for over 95% or the
546 total". Can you please add a reference? Is that also true at your site?

547 ***Response:***

548 We have added references in the manuscript. During the sampling period (March 2014 to
549 June 2015 and May 2016 to December 2016), the GOM concentration is 14.81 ± 13.21 pg m⁻³
550 and GEM concentration is 2.15 ± 0.94 ng m⁻³. Thus, the GOM concentration accounted for
551 0.68% and the conclusion in the reference is also true at our site. We also added reference in

552 our manuscript as below.

553 “In the atmosphere, Hg mainly presents as GEM, accounting for over 95% of the total in
554 most observation sites (Fu et al., 2015; Li et al., 2016; Zhang et al., 2017).”

555 **See the revised manuscript at line 49**

556

557 **Comment 4:**

558 Line 61-62: "(: :) there is no official national monitoring network of atmospheric Hg". Out of
559 curiosity, what is the current status of the Asian-Pacific Mercury Monitoring Network
560 (<http://nadp.sws.uiuc.edu/newIssues/asia/>)? Do you think that Chinese sites will be included?

561 **Response:**

562 Thanks for the comment. Asian-Pacific Mercury Monitoring Network (APMMN) was
563 established in 2013 with founding countries and regions including the U.S, China Taiwan,
564 Thailand, Vietnam, Indonesia, Japan, Korea and Canada
565 (<http://apmmn.org/AboutAPMMN.html>). APMMN has been monitoring atmospheric mercury
566 deposition in the Asia-Pacific region and holds annual meetings since 2013. Currently, there is
567 no monitoring site of mainland China in the APMMN (see the Figure R2).



568 Figure R2. The participating country of APMMN (<http://apmmn.org/AboutAPMMN.html>)

569 Considering the large Hg emissions in mainland China, including the Chinese sites into the
570 monitoring network will help for the research of Hg behavior in the regional or global scale.
571 However, nearly all mercury monitoring sites belong to individual researchers in China
572 currently. Therefore, whether the Chinese sites will be included mainly depend on multiple
573 factors such as individual interests and potential benefit. We also revised our expression in the
574 manuscript as below.

575 “For the developing countries such as China, limited atmospheric Hg observations have been
576 carried out (Fu et al., 2008b; Zhang H et al., 2016; Hong et al., 2016) and there is no official
577 national monitoring network of atmospheric Hg in mainland China.”

578 **See the revised manuscript at line 63 - 66**

579

580 ***Comment 5:***

581 Lines 64-67: "Atmospheric Hg emissions in China accounted for 27% of the global total in
582 2010 (UNEP, 2013), which led to high air Hg concentrations in China. Therefore, atmospheric
583 Hg observations in China are critical to understand the Hg cycling at both regional and global
584 scale". Please define "high" air Hg concentrations. Additionally, in order to emphasize the fact
585 that observations in China are critical to understand the Hg cycling on a global scale, you could
586 perhaps add a sentence about 1) future projections (e.g., Chen et al., 2018; Pacyna et al., 2016),
587 and 2) long-range transport of Chinese emissions to other regions (e.g., Chen et al., 2018;
588 Corbitt et al., 2011; Sung et al., 2018).

589 ***Response:***

590 Hg concentration in remote site in China and Northern Hemisphere are compared to illustrate
591 the level of Hg pollution in China. Long-range transport and future projections are added to
592 emphasize observation in China are critical to understand Hg cycling on a global scale.

593 The related paragraph is revised as below.

594 “China contributes to the largest Hg emissions in the world and will continue to be one
595 significant Hg emitter for global Hg emissions in the coming future (UNEP, 2013, Wu et al.,
596 2016, Chen et al., 2018; Pacyna et al., 2016). Large Hg emissions in China have led to the
597 average air Hg concentrations of $2.86 \pm 0.95 \text{ ng m}^{-3}$ (in the range of 1.60-5.07 ng m^{-3}) at the

598 remote sites in China (Fu et al., 2015). Such Hg concentration level is approximately 1.3 ng m⁻³
599 ³ higher than the background concentration of GEM in Northern Hemisphere (Zhang et al.,
600 2016;Sprovieri et al., 2017;Fu et al., 2015). In addition, the large Hg emissions in China will
601 also impact the air Hg concentrations in East Asia and even North America through long-range
602 transport (Sung et al., 2018;Zhang et al., 2017).”

603 **See the revised manuscript at line 67 – 75.**

604

605 ***Comment 6:***

606 Lines 93-94: "we used Tekran 2537X/1130/1135 instruments to monitor speciated Hg in the
607 atmosphere". I wonder why GOM and PBM concentrations are not reported in the manuscript.

608

609 ***Response:***

610 We didn't report the GOM and PBM concentration because the main purpose of this
611 manuscript is to validate the anthropogenic Hg emissions reduction through observation data.
612 The Chongming site is a background site. Considering the stability of GEM in the air, we
613 choose GEM as an index to reflect the emission control effect. In addition, the method we
614 developed to explain the GEM trend is not applicable for GOM and PBM. Except emissions,
615 we think the potential reactions in the air are more significant factors for GOM and PBM. But
616 we need more evidence to prove our assumptions. Therefore, we deleted the discussion of GOM
617 and PBM in our final manuscript.

618

619 If concentrations were recorded, it would be interesting to discuss the results. Do you also see
620 a decreasing trend from 2014 to 2016? From 1978 to 2014, the fractions of GEM and PBM
621 decreased, while the GOM emission share gradually increased (Wu et al., 2016). What about
622 the speciation of emissions since 2014? Can you observe a trend in GOM/PBM concentrations?

623

624 ***Response:***

625 Yes. The downward trend of PBM concentration was observed to decrease from 2014 (24.51
626 ± 43.31 pg m⁻³) to 2016 (22.07 ± 30.55 pg m⁻³), which was also consistent with the downwawrd

627 trend of GEM. However, the GOM concentration increased from $(15.41 \pm 16.02 \text{ pg m}^{-3})$ in
628 2014 to $(18.97 \pm 9.28 \text{ pg m}^{-3})$ in 2016. Speciated Hg emissions were showed in Table R1. All
629 speciated Hg emissions have decreased since 2014 in the YRD regions. However, we observed
630 significant GEM decreasing. But the decrease of GOM and PBM was quite slight.

631

632 **Table R1.** Speciated Hg emissions in YRD region and concentration at Chongming island in
633 2014 and 2016

Year	Emission			Concentration		
	GEM (t)	GOM (t)	PBM (t)	GEM (ng m^{-3})	GOM (pg m^{-3})	PBM (pg m^{-3})
2014	34.26	30.41	1.50	2.68	15.41	24.51
2016	27.65	29.16	1.39	1.60	18.97	22.07

634

635 Alternately, did you have issues with the speciation unit? It is quite common and I would
636 appreciate an open discussion about that and associated analytical uncertainties. What kind of
637 issues did you encounter? Are you confident that you collected and analyzed GEM (vs. TGM)
638 during the entire experiment? Was the instrumental setup exactly the same during the entire
639 experiment? If not, how can you compare GEM concentrations without discussing analytical
640 uncertainties? See major comment.

641

642 Yes, we encountered issues with the speciation unit. The Tekran 2537X was consistent and
643 in good condition during the sampling period. There was no data in January and February in
644 2016 due to equipment failure. The Tekran 1130/1135 was accidentally rained by rain, so there
645 was no data of speciated mercury between July 2015 and April 2016. From July 2015 to April
646 2016, we used Tekran 2537X only with PTFE filter to monitor atmospheric mercury. The
647 average concentration of GOM during sampling period (March, 2014 to June 2015, May 2016
648 to December 2016) was $14.81 \pm 13.21 \text{ pg m}^{-3}$, which is approximately 1% of GEM
649 concentration. Thus, the GEM concentrations were approximated to TGM concentrations July
650 5, 2015 to April 30 2016 when the speciation unit does not work, as most of other studies have
651 done (Slemr et al., 2015; Sprovieri et al., 2016). In addition, we have added discussion about
652 the analytical uncertainties to point out potential impact.

653 The manuscript was revised as below.

654 “From July 5, 2015 to April 30 2016, the Tekran 1130/1135 speciation unit was damaged by
655 the rainstorm, the Tekran 2537X were operated without speciation units but with PTFE filter to
656 protect the instrument from particles and sea salt. Therefore, the observed concentrations during
657 July 2015-April 2016 were TGM concentrations indeed. However, the GOM concentrations at
658 Chongming Island accounted for less than 1% of TGM (TGM=GOM+GEM). Thus, the GEM
659 concentrations were approximated to TGM concentrations from July 2015 to April 2016.”

660 **See the revised manuscript at line 108 – 114**

661 “In our research, random uncertainties of individual measurement had been averaged out and
662 the systematic uncertainties need to be considered. The overall practically achievable
663 systematic uncertainty would be 10% considering that the instrument was not in ideal
664 performance (Slemr et al., 2015; Steffen et al., 2012). For example, slow deactivation of the
665 traps, contamination of the switching valves and leaks would increase the uncertainties but were
666 difficult to quantify (Slemr et al., 2015;Steffen et al., 2012). Because of the consistency of
667 instrument and the quality assurance/quality control have been paid special attention to during
668 the sampling campaign, the systematic differences of instrument did not affect the huge
669 variation between 2014 and 2016.”

670 **See the revised manuscript at line 122 – 129**

671

672 ***Comment 7:***

673 Lines 103-104: "The impactor plates and quartz filter were changed in every two weeks. The
674 quartz filter was changed once a month". Did you change the quartz filter every two weeks or
675 once a month?

676 ***Response:***

677 Yes, the impactor plates, Teflon filter and quartz filter were changed in every two weeks.
678 The soda lime was changed once a month. We have corrected this sentence in the revised
679 manuscript as below.

680 “The impactor plates and quartz filter were changed in every two weeks. The soda lime was
681 changed once a month.”

682 **See the revised manuscript at line 119 – 120**

683

684 **Comment 8:**

685 Line 106: "During the sampling campaigns, PM_{2.5}, O₃, NO_x, CO and SO₂ were monitored".

686 Why aren't you discussing the data, especially SO₂, NO_x, PM_{2.5} while your main conclusion is

687 that Hg decreasing trend in due to air pollution control policies targeting SO₂, NO_x, and PM_{2.5}.

688 I agree that you present emissions inventories, but I would really appreciate to see a real

689 interpretation and discussion of these data. Do you also observe a decreasing trend? See major

690 comment.

691 **Response:**

692 To further verify the cause of downward trend of atmospheric Hg, we give the emission

693 inventory (Table S6) and concentrations (Table S5) of other air pollutants in the studied regions

694 in both 2014 and 2016. Both the emissions and concentrations of SO₂, NO₂, and PM showed a

695 decreasing trend, which is used to support that "air pollution control policies targeting SO₂,

696 NO₂, and PM reductions had significant co-benefits on atmospheric Hg".

697 "Table 3 showed the detailed data of the three classifications. From 2014 to 2016, the whole

698 China region (NCP, SW-YRD) contributed to 70% of GEM decline at Chongming Island.

699 Considering downward trend of emission inventory and atmospheric pollutant from 2014 to

700 2016 in NCP and SW-YRD region (Table S5, Table S6), the reason of downward trend can be

701 attributed to the effectiveness of existing air pollution control measures in China (SC, 2013;

702 MEP, 2014)."

703 **See the revised manuscript at line 375 – 379**

704

705 **Table S5.** The annual concentration of SO₂, NO_x, O₃ and PM_{2.5} at Chongming site, NCP, and

706 SW-YRD regions

Year		2014			2016			Change		
Pollutants	Region	NCP	SW-YRD	Chongming	NCP	SW-YRD	Chongming	NCP	SW-YRD	Chongming
PM _{2.5} (µg m ⁻³)		71.93	53.05	25.09	60.75	44.75	23.89	-16%	-16%	-5%
SO ₂		34.52	21.01	1.60	24.37	16.40	1.47	-29%	-22%	-8%

($\mu\text{g m}^{-3}$)									
NO ₂	45.07	34.34	12.62	41.55	34.40	10.84	-8%	0%	-14%
($\mu\text{g m}^{-3}$)									
O ₃	60.29	56.27	41.70	61.84	60.92	44.38	3%	8%	6%
($\mu\text{g m}^{-3}$)									
GEM	No data		2.68	No data		1.60		No data	-40%
(ng m^{-3})									

707 Note: According to the contribution of trajectory, the dominant provinces in the NCP region
708 included Beijing, Tianjin, Hebei, Shandong and Liaoning province. The SW-YRD mainly
709 contained Shanghai, Zhejiang, Jiangsu, Jiangxi and Anhui province.

710

711 **Table S6.** Emission inventories of the main pollutants from the studied regions in 2014 and
712 2016

Air pollutants	2014		2016		Decline proportion	
	NCP	SW-YRD	NCP	SW-YRD	NCP	SW-YRD
PM _{2.5} (kt)	2019	1209	1849	1109	-8%	-8%
NO _x (kt)	5697	4022	5424	3855	-5%	-4%
SO ₂ (kt)	3780	1993	3450	1780	-9%	-11%
GEM (t)	118	72	103	67	-13%	-7%

713 Note: According to the contribution of trajectory, the dominant provinces in the NCP region
714 included Beijing, Tianjin, Hebei, Shandong and Liaoning province. The SW-YRD mainly
715 contained Shanghai, Zhejiang, Jiangsu, Jiangxi and Anhui province.

716

717 **Comment 9:**

718 Lines 173-175: "Besides, this method required similar meteorological conditions of the periods
719 participated in comparison so as to reduce the interference from meteorology". I am not sure I
720 understand this sentence. Do you mean that you used similar meteorological data in 2014 and
721 2016 to compute the back-trajectories? Or are you referring to the fact that meteorological
722 conditions were pretty much similar in 2014 and 2016 (lines 266-270)?

723 **Response:**

724 Thanks for the comments. Yes, this sentence is referring to the fact that meteorological
725 conditions were pretty similar in 2014 and 2016. We have revised the sentence as suggested to
726 make it easier to understand.

727 "Besides, meteorological conditions were pretty similar in 2014 and 2016 so as to reduce the
728 interference from meteorology (Table S2).

729 **See the revised manuscript at line 200 – 201**

730

731 **Comment 10:**

732 Lines 188: "For small emission sectors (: : :)". Which ones?

733 **Response:**

734 We have added the explanation of small emission sectors in the revised manuscript as below.

735 "The emission sectors included coal-fired power plants, coal-fired industrial boilers,
736 residential coal-combustion, cement clinker production, iron and steel production, mobile oil
737 combustion, and other small emission sectors (eg., zinc smelting, lead smelting, municipal solid
738 incineration, copper smelting, aluminum production, gold production, other coal combustion,
739 stationary oil combustion, and cremation)."

740 **See the revised manuscript at line 208-212.**

741

742 **Comment 11:**

743 Lines 193-194: "The average concentrations of GEM in 2014 and 2016 were (: : :)". What about
744 the mean concentration in 2015? Additionally, are the average annual concentrations actually
745 referring to March-December? If so, please add something like "The average concentrations of
746 GEM in 2014 (Mar-Dec) and 2016 (Mar-Dec) were (: : :)".

747 **Response:**

748 The average concentration of GEM in 2015 was $2.14 \pm 0.82 \text{ ng m}^{-3}$. And we have added the
749 concentration of 2015 and remark in the revised manuscript.

750 "The average concentrations of GEM in 2014 (March to December), 2015 and 2016 (March
751 to December) were $2.68 \pm 1.07 \text{ ng m}^{-3}$, $2.14 \pm 0.82 \text{ ng m}^{-3}$, and $1.60 \pm 0.56 \text{ ng m}^{-3}$, respectively."

752 **See the revised manuscript at line 226 – 227**

753

754 **Comment 12:**

755 Lines 194-195: How does it compare to concentrations reported in Sprovieri et al. (2016)?

756 **Response:**

757 *t* test was used to compare the GEM concentration at Chongming and background
758 concentration of Northern Hemisphere. The *p* value ($p < 0.01$) of the *t* test were added in the
759 revised manuscript as below.

760 “The GEM concentrations in 2014 ($2.68 \pm 1.07 \text{ ng m}^{-3}$) were higher (t test, $p < 0.01$) than the
761 Northern Hemisphere back-ground concentration (about 1.5 ng m^{-3}) (Sprovieri et al., 2010) and
762 those measured in other remote and rural locations in China (Zhang H et al., 2015; Fu et al.,
763 2008a; Fu et al., 2009).”

764 **See the revised manuscript, line 229 – 231**

765

766 ***Comment 13:***

767 Lines 199-200: "During this period, monthly GEM concentrations showed a significant
768 decrease with a rate of $-0.60 \text{ ng/m}^3/\text{yr}$ ". Table 1 refers to TGM concentrations, not GEM.
769 Additionally, as mentioned earlier, the rate is $-0.52 \text{ ng/m}^3/\text{yr}$ in Table 1. Please, try to be
770 consistent throughout the manuscript.

771 ***Response:***

772 Thanks for the comments. It is a typo. We have gone through the whole paper so as to make
773 the manuscript consistent.

774

775 ***Comment 14:***

776 Lines 201-216: To me, "GEM" and "TGM" are not interchangeable (see previous comment).
777 While the difference between TGM and GEM is usually smaller than 1% (Soerensen et al.,
778 2010), it might not be the case everywhere. What is the fraction of GOM at your site? I would
779 appreciate a discussion on analytical uncertainties and instrumental setups.

780 ***Response:***

781 We agree that the GEM and TGM are not always interchangeable. The average concentration
782 of GOM during sampling period was $14.81 \pm 13.21 \text{ pg m}^{-3}$, which was less than 1% of TGM.
783 Thus, the GEM concentrations were approximated to TGM concentrations July 5, 2015 to April
784 30 2016 when the speciation unit does not work, as most of other studies have done (Slemr et
785 al., 2015; Sprovieri et al., 2016). We have pointed out this in the revised manuscript.

786 A discussion on analytical uncertainties and instrumental setups has been added in the following
787 text as below.

788 “From July 5, 2015 to April 30 2016, the Tekran 1130/1135 speciation unit was damaged by
789 the rainstorm, the Tekran 2537X were operated without speciation units but with PTFE filter to

790 protect the instrument from particles and sea salt. Therefore, the observed concentrations during
791 July 2015-April 2016 were TGM concentrations indeed. However, the GOM concentrations at
792 Chongming Island accounted for less than 1% of TGM (TGM=GOM+GEM). Thus, the GEM
793 concentrations were approximated to TGM concentrations from July 2015 to April 2016.”

794 **See the revised manuscript at line 108 – 114**

795 “In our research, random uncertainties of individual measurement had been averaged out and
796 the systematic uncertainties need to be considered. The overall practically achievable
797 systematic uncertainty would be 10% considering that the instrument was not in ideal
798 performance (Slemr et al., 2015; Steffen et al., 2012). For example, slow deactivation of the
799 traps, contamination of the switching valves and leaks would increase the uncertainties but were
800 difficult to quantify (Slemr et al., 2015; Steffen et al., 2012). Because of the consistency of
801 instrument and the quality assurance/quality control have been paid special attention to during
802 the sampling campaign, the systematic differences of instrument did not affect the huge
803 variation between 2014 and 2016.”

804 **See the revised manuscript at line 124 – 129**

805

806 The sentence "at the Cape Point of South Africa, GEM concentrations decreased from 1.35
807 ng/m³ in 1996 to 0.9 ng/m³ in 2008" is not entirely true. A downward trend has been observed
808 from 1996 to 2005, while an upward one is observed since 2007 (Martin et al., 2017; Slemr et
809 al., 2015).

810 **Response:**

811 We have revised our expression about observation trend in Cape Point as follows

812 “In South Africa, annual average GEM concentration at Cape Point decreased from 1.29 ng m⁻³
813 ³ in 1996 to 1.19 ng m⁻³ in 2004 (Slemr et al., 2008) and were increasing from 0.93 ng m⁻³ in
814 2007 (Slemr et al., 2015) until 2016 (Martin et al, 2017).”

815

816 Additionally, the instrumental setup changed: a manual amalgamation technique was used from
817 1995 to 2004 while a Tekran instrument has been used since 2007 (Martin et al., 2017). It might
818 also be the case at other stations in Table 1. How does it influence the various trends reported
819 in Table 1?

820 **Response:**

821 Table 1 was moved to supporting information (Table S4) so as to focus on our topic. In the
822 Table S4, all the stations used Tekran instruments except for the monitoring in South Korea.
823 The instrument of Canadian sites were maintained by the Environment Canada- developed
824 Research Data Management and Quality Assurance System (RDMQ). At Zeppelin, the
825 instrument maintenance were carried out by the protocols of Norwegian mercury monitoring
826 program. Instruments at these places have been maintained under the guidance of similar
827 quality control criteria. In South Korea, the concentration of TGM were measured using an
828 automatic on-line analytical system called a AM-series analyzer. Although the instruments used
829 in the stations listed in the Table 1 were not totally the same, the instruments at each site
830 remained unchanged during the monitoring period. Therefore, the downward trend at different
831 sites can be compared in the Table S4. We have revised the Table S4 and give expression about
832 the different instrument in the revised manuscript.

833 “All the stations in Table S4 used Tekran instruments except for the observation in South
834 Korea. Different instruments could cause potential differences in the observation, but they were
835 comparable and did not affect the conclusion of comparison in downward trend (Slemr et al.,
836 2015; Sprovieri et al., 2016).”

837 **See the revised manuscript at line 249 - 252**

838 **Table S4.** Historical variation trends of atmospheric Hg in previous studies

Monitoring site	Duration	TGM trend (pg m ⁻³ yr ⁻¹)	Variation trend	Site description	Monitoring instrument	References
Alert, Canada	2000-2009	-13(-21,0)	-0.9% y ⁻¹	Remote	2537A	Cole et al. 2013
Kuujuarapik, Canada	2000-2009	-33(-50,-18)	-2.1% y ⁻¹	Remote	2537A	Cole et al. 2013
Egbert, Canada	2000-2009	-35(-44,-27)	-2.2% y ⁻¹	Remote	2537A	Cole et al. 2013
Zeppelin Stn, Norway	2000-2009	+2(-7,+12)	-	Remote	2537A	Cole et al. 2013
St.Anicet, Canada	2000-2009	-29(-31,-27)	-1.9% y ⁻¹	Remote	2537A	Cole et al. 2013
Kejimkujik, Canada	2000-2009	-23(-33,-13)	-1.6% y ⁻¹	Remote	2537A	Cole et al. 2013

Head, Ireland	1996- 2009	-	$-1.3 \pm 0.2\% \text{ y}^{-1}$	Rural	2537A	Weigelt et al. 2015
Yong San, South Korea	2004- 2011	No trend ($3.54 \pm 1.46 \text{ ng m}^{-3}$)		Urban	AM-3	Kim et al. 2016
Yong San South Korea	2013- 2014	Decrease to $2.34 \pm 0.73 \text{ ng m}^{-3}$			AM-3	Kim et al. 2016
Mt. Changbai	2013- 2015	Decrease from 1.74 ng m^{-3} to 1.58 ng m^{-3}		Remote	2537B	Fu et al. 2015
Chongming Island, China	2014- 2016	-600	$-29.4\%/y$	Remote	2537X	This study

839

840 **Comment 15:**

841 Lines 212-214: "The decreasing trend observed in our study was accordant with the
842 unpublished data in Mt. Changbai during 2014-2015 cited in the review of Fu et al. (2015). But
843 much sharper decrease of Hg concentrations was observed in our study". Aren't the data at Mt.
844 Changbai you are referring to in Sprovieri et al. (2016)? What is the trend at that site? Why
845 isn't included in Table 1?

846 **Response:**

847 The data of Mt. Changbai reported by Sprovieri et al. (2016) is the observation in 2013. The
848 observation period is not in the range of our study period. Therefore, we cited the data reported
849 by Fu et al.(2015), where the observation is in 2014-2015.

850 "The decreasing trend observed in our study was accordant with the data in Mt. Changbai
851 during 2014-2015 cited in the review of Fu et al. (2015). The atmospheric mercury at
852 Chongming was influenced by and in turn reflected regional mercury emission and cycle.
853 Although the decline in atmospheric mercury was observed in many sites of the Northern
854 Hemisphere, much sharper decrease of Hg concentrations was observed in our study."

855 **See the revised manuscript at line 262 - 267**

856

857 **Comment 16:**

858 Line 224: Are you referring to Figure 2?

859 **Response:**

860 Refer to figure 3 in our revised manuscript. We have corrected this in the revised manuscript.

861

862 **Comment 17:**

863 Lines 225-227: Is that based on the _3 years of data?

864 **Response:**

865 Figure 3 is calculated based on the 3 years data. We have revised it in the manuscript as
866 below.

867 “According to the decomposition result (Figure 2c), we observed strong seasonal cycle at
868 Chongming. The GEM concentrations were highest in July and lowest in September, so GEM
869 concentrations in the same month from different years were averaged to understand the
870 detrended seasonal circle (Figure 3).”

871 **See the revised manuscript at line 270 - 276**

872

873 **Comment 18:**

874 Line 234: "The higher Hg concentrations in cold seasons in Mt. Ailao and Mt. Waliguan (: : :)".

875 You say above that concentrations are lower in the cold season at these sites. This is confusing.

876 **Response:**

877 Sorry for the mistakes. We have revised the manuscript as below.

878 “The higher Hg concentrations in cold seasons in Mt. Leigong were mainly explained by coal-
879 combustion for urban and residential heating during cold seasons. Whereas, increasing solar
880 radiation and soil/air temperature dominate the higher Hg concentrations in Mt. Ailao.”

881 **See the revised manuscript at line 283- 286**

882

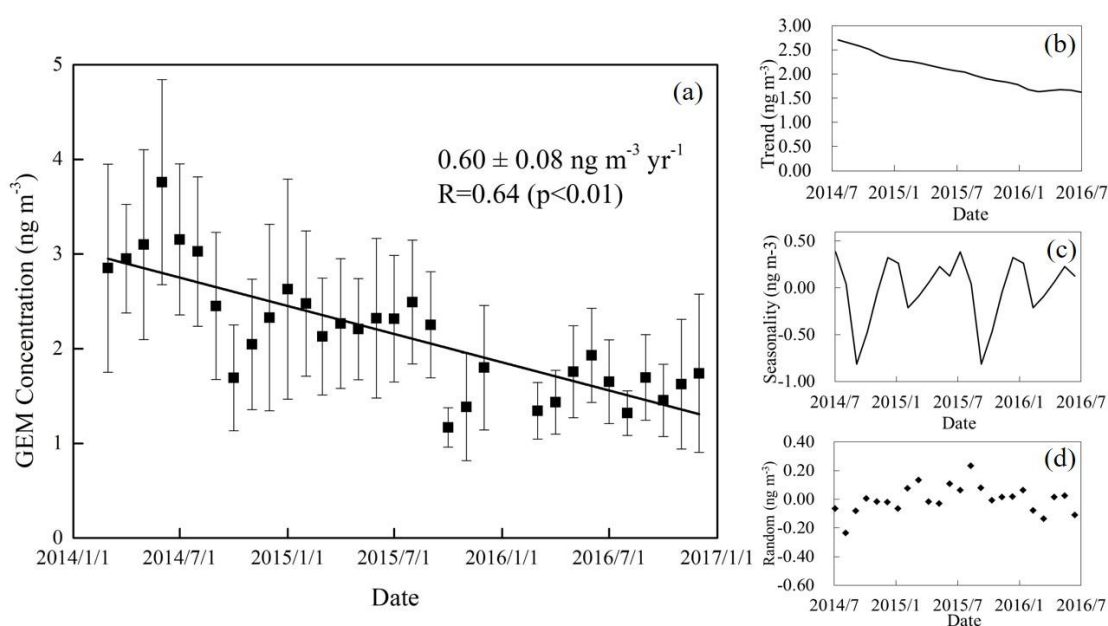
883 **Comment 19:**

884 Line 250-251: "Therefore, we supposed that the seasonal cycle of GEM concentrations was
885 dominated by natural emissions". How can you explain that the seasonal cycle is more
886 pronounced in 2014 than in 2016? See major comment.

887 **Response:**

888 The seasonal variation was more pronounced in 2014 can attribute to the lower wet
889 deposition and GEM oxidation. On one aspect, as a costal site, the Chongming island is

890 abundant with •OH. The increase of O₃ concentration from the summer of 2014 to 2016 may
 891 contribute to a higher oxidation of GEM in 2016. On another aspect, higher wet Hg deposition
 892 in summer is approximately 6.6 times of that in the winter at Chongming (Zhang et al., 2010).
 893 Meanwhile, the rainfall in 2016 summer (546 mm) was higher than the rainfall in 2014 (426
 894 mm). Therefore, the higher oxidation and wet deposition rate of mercury in the summer of 2016
 895 will reduce the concentration difference between summer and winter, which lead to a less
 896 pronounced seasonal variation in 2016.
 897



898

899 **Figure 2.** Monthly average GEM concentrations during the studied period (a) observed monthly
 900 GEM concentrations (b) GEM trend after decomposition (c) GEM seasonality after
 901 decomposition (d) GEM random after decomposition

902 Note: The observed concentrations during July 2015-April 2016 were TGM concentrations
 903 indeed due to the problems of Tekran 1130/1135. However, the GOM concentrations at
 904 Chongming island accounted for less than 1% of TGM. Thus, the GEM concentrations were
 905 approximated to TGM concentrations during July 2015-April 2016.

906 “From Figure 2, we also observed more pronounced seasonal variation in 2014, which can
 907 be attributed to the lower wet deposition and GEM oxidation. On one aspect, as a costal site,
 908 the Chongming Island is abundant with •OH. The increase of O₃ concentration from the summer
 909 of 2014 to 2016 may contribute to a higher oxidation of GEM in 2016. On another aspect,

910 higher wet Hg deposition in summer is approximately 6.6 times of that in the winter at
911 Chongming (Zhang et al., 2010). Meanwhile, the rainfall in 2016 summer (546 mm) was higher
912 than the rainfall in 2014 (426 mm). Therefore, the higher oxidation and wet deposition rate of
913 Hg in the summer of 2016 will reduce the concentration difference between summer and winter,
914 which lead to a less pronounced seasonal variation in 2016. Meanwhile, the higher oxidation
915 and wet deposition in 2016 also contributed to the downward trend of GEM by reducing the
916 seasonality in spring and summer (Figure S3).”

917 **See the revised manuscript at line 313 - 323**

918

919 ***Comment 20:***

920 Lines 275-276: "This decline may be contributed by the downward trend of GEM
921 concentrations in north hemisphere". Please, elaborate on this idea. I don't really understand
922 what you mean here.

923 ***Response:***

924 Sorry for the obscure expression. The decline of PSCF value means that East China Sea has
925 less contribution to Chongming in 2016. The potential reason of the decline on PSCF value in
926 the East China Sea may be attributed to the reduction of emissions in Japan and Korea. The
927 downward trend in Japan and Korea will lead to clean air mass transport from Japan and Korea
928 to East China Sea and then to Chongming. We have revised the manuscript as below:

929 “The decline from the East China Sea may be contributed by the downward trend of GEM
930 concentrations in South Korea and Japan (Kim et al., 2016; Kim et al., 2013), where the
931 anthropogenic Hg emissions of Japan and South Korea have been reduced by 13% and 4%
932 during 2010-2015, respectively (UNEP 2013; UNEP 2018). The air mass from Japan and South
933 Korea would pass through the East China Sea to Chongming.”

934 **Table R2.** Total Hg emission from Japan and South Korea in 2010 and 2015

Country	Mercury emissions (t)		Decline	Reference
	2010	2015		
Japan	17.07	14.86	-13%	UNEP Technical Report (2013)
South Korea	7.32	7.01	-4%	UNEP Technical Report (2018)

935 **See the revised the manuscript at line 331-335**

936

937 ***Comment 21:***

938 Lines 315-325: Do you get the same results if you perform this analysis on SO₂, NO_x, and PM
939 concentrations?

940 ***Response:***

941 The SO₂, NO_x and PM_{2.5} concentrations at Chongming island also show downward trend.
942 However, such kind of analysis is not so suitable for SO₂, NO_x, and PM_{2.5} due to the following
943 reasons. First, the residential time of SO₂, NO_x, and PM_{2.5} is 2-4 d, 8-10d, and several days to
944 few weeks, respectively (Pirrone, et al., 1996, Seinfeld, Spyros, 2016). Such residential time is
945 much shorter than that for Hg⁰. Second, SO₂, NO_x and PM_{2.5} are more reactive in the
946 atmosphere compared with Hg⁰ (Pirrone, et al., 1996, Seinfeld, Spyros, 2016).

947

948 ***Comment 22:***

949 Line 318: 34% should be 35% according to Table 4. Additionally, how can you explain this
950 result? Is there a decline in anthropogenic emissions and a GEM decreasing trend in this region
951 (China Sea, Japan, South Korea) as well? Cluster EAST explains 35% of the decline, i.e., 0.35
952 x 0.52 = 0.182 ng/m³/yr. Is that consistent with trends reported in this region (e.g., Kim et al.,
953 2016)?

954 ***Response:***

955 Yes. This is a mistake that 34% should be 35% in the original manuscript.

956 However, we have changed the definition of cluster according to the suggestion. The NCP
957 region, SW-YRD region, and ABROAD region causes 26%, 44%, and 30% for GEM decline,
958 respectively. The whole China region (NCP, SW-YRD) contributed to 70% of GEM decline at
959 Chongming Island while ABROAD region contributed to 30%. The decline in NCP and SW-
960 YRD indicated effective air pollution control policy in China since 2013. The decline in
961 ABROAD region was originated from GEM decline in South Korea and Japan.

962 The decline in Chongming was consistent with the decline in anthropogenic emission and a
963 GEM decreasing trend in the ABROAD region. In South Korea, the decline of GEM at Seoul
964 can be calculated as 0.47 ng m⁻³ yr⁻¹ from 2011 to 2013 (Kim, et al., 2016, Kim, et al., 2013).
965 In Japan, there is no published data about long term trend since 2010. But the emission

966 inventory of Japan decreased from 2010 to 2015 (Table R2). Therefore, the decline in
967 ABROAD can be attributed to the decline in South Korea and Japan.

968 **Table R2.** Total Hg emission from Japan and South Korea in 2010 and 2015

Country	Mercury emissions (t)		Decline	Reference
	2010	2015		
Japan	17.07	14.86	-13%	UNEP Technical Report (2013)
South Korea	7.32	7.01	-4%	UNEP Technical Report (2018)

969

970 We also revised the manuscript as below.

971 “The decline from the East China Sea may be contributed by the downward trend of GEM
972 concentrations in South Korea and Japan (Kim et al., 2016; Kim et al., 2013), where the
973 anthropogenic Hg emissions of Japan and South Korea have been reduced by 13% and 4%
974 during 2010-2015, respectively (UNEP 2013; UNEP 2018). The air mass from Japan and South
975 Korea would pass through the East China Sea to Chongming.”

976 **See the revised manuscript at line 331 -335**

977

978 **Comment 23:**

979 Lines 321-323: "We also noted that the largest decline of Hg concentrations was observed in
980 the cluster SW, which indicated more effective air pollution control in the regions where the air
981 mass of the cluster SW passed". What about the seasonality of GEM concentrations in the
982 various clusters (NW, SW and EAST)? Could a difference in seasonality explain the observed
983 Hg decline?

984 **Response:**

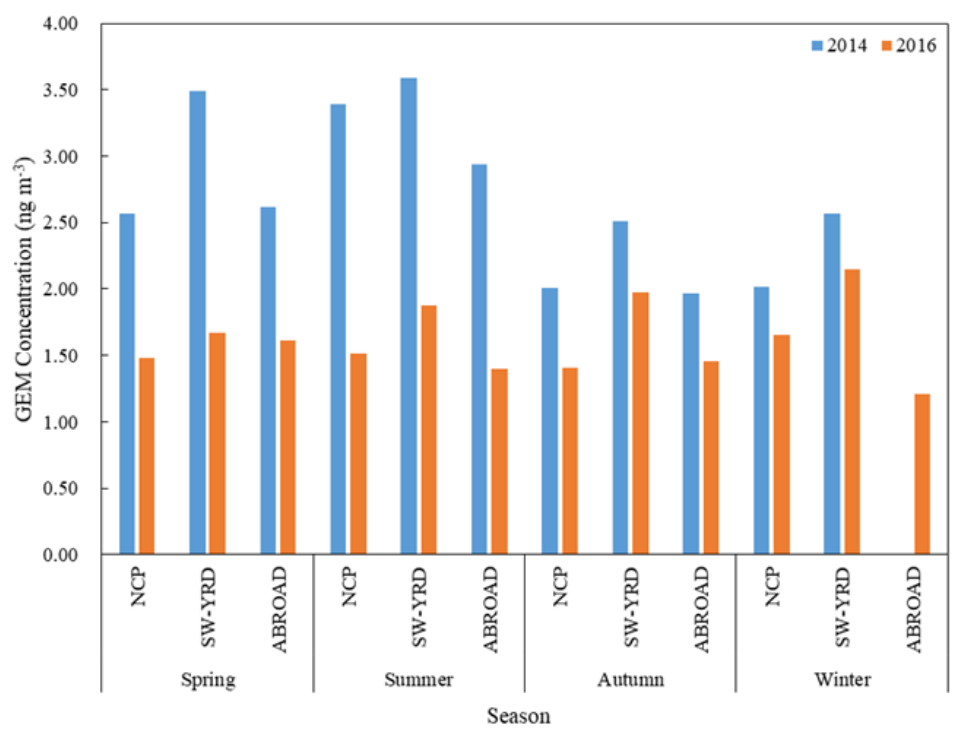
985 The seasonality of GEM concentration in the various clusters was showed in Figure S3. In
986 our revised manuscript, cluster NW, SW and EAST were modified to cluster NCP, SW-YRD
987 and ABROAD. The seasonality of cluster NCP, SW-YRD and ABROAD were similar to the
988 seasonality at Chongming. The GEM concentration of different clusters reached the highest in
989 the summer of 2014. And the seasonality in 2014 for the three clusters was more pronounced
990 than their seasonality in 2016.

991 The seasonality also explained the observed decline. From 2014 to 2016, all the clusters

992 declined in all season. In 2014, the seasonality was more pronounced than the seasonality in
 993 2016. It can be attributed to the higher oxidation of GEM and higher wet deposition in 2016.
 994 The smaller seasonal variation also had an effect on the decline. We revised our expression in
 995 the revised manuscript.

996 “Therefore, the higher oxidation and wet deposition rate of mercury in the summer of 2016
 997 will reduce the concentration difference between summer and winter, which lead to a less
 998 pronounced seasonal variation in 2016. Meanwhile, the higher oxidation and wet deposition in
 999 2016 also contributed to the downward trend by reducing the seasonality of spring and summer
 1000 (Figure S3).”

1001 **See the revised manuscript in line 319 – 323.**



1002 **Figure S3.** The seasonality of GEM concentration in the NCP, SW-YRD and ABROAD (No
 1003 trajectory transport though ABROAD in winter of 2014)
 1004

1005 **See the revised manuscript at Figure S3.**

1006
 1007 **Comment 24:**

1008 Figure 3: Could you please add the standard deviations? Is that the average over several years?

1009 **Response:**

1010 We have revised as suggested. It is the average in the three years. We also give expression in

1011 the manuscript as below.

1012 “According to the decomposition result (Figure 2c), we observed strong seasonal cycle at
1013 Chongming. The GEM concentrations were highest in July and lowest in September, so GEM
1014 concentrations in the same month from different years were averaged to understand the
1015 detrended seasonal circle (Figure 3). The error bars in the Figure 3 meant the standard deviation
1016 of the monthly average.”

1017 **See the revised manuscript in line 270– 274.**

1018

1019 **References:**

- 1020 Chen, L., Zhang, W., Zhang, Y., Tong, Y., Liu, M., Wang, H., Xie, H., and Wang, X.: Historical
1021 and future trends in global source-receptor relationships of mercury, *Sci Total Environ*, 610-611,
1022 24-31, 10.1016/j.scitotenv.2017.07.182, 2018.
- 1023 Cheng, Y. F., Zheng, G. J., Wei, C., Mu, Q., Zheng, B., Wang, Z. B., Gao, M., Zhang, Q., He, K.
1024 B., Carmichael, G., Poschl, U., and Su, H.: Reactive nitrogen chemistry in aerosol water as a
1025 source of sulfate during haze events in China, *Science Advances*, 2, no. 12, e1601530,
1026 10.1126/sciadv.1601530, 2016.
- 1027 Fu, X. W., Zhang, H., Yu, B., Wang, X., Lin, C. J., and Feng, X. B.: Observations of atmospheric
1028 mercury in China: a critical review, *Atmospheric Chemistry and Physics*, 15, 9455-9476,
1029 10.5194/acp-15-9455-2015, 2015.
- 1030 Li, S., Gao, W., Wang, S. X., Zhang, L., Li, Z. J., Wang, L., and Hao, J. M.: Characteristics of
1031 Speciated Atmospheric Mercury in Chongming Island, Shanghai, *Environmental Science* 37, 3290
1032 - 3299, 2016.
- 1033 Kim, K.-H., Yoon, H.-O., Brown, R. J. C., Jeon, E.-C., Sohn, J.-R., Jung, K., Park, C.-G., and
1034 Kim, I.-S.: Simultaneous monitoring of total gaseous mercury at four urban monitoring stations in
1035 Seoul, Korea, *Atmospheric Research*, 132-133, 199-208, 10.1016/j.atmosres.2013.05.023, 2013.
- 1036 Kim, K.-H., Brown, R. J. C., Kwon, E., Kim, I.-S., and Sohn, J.-R.: Atmospheric mercury at an
1037 urban station in Korea across three decades, *Atmospheric Environment*, 131, 124-132,
1038 10.1016/j.atmosenv.2016.01.051, 2016
- 1039 Pirrone N, Keeler G J, Nriagu J O. Regional Differences in Worldwide Emissions of Mercury to
1040 the Atmosphere. *Atmospheric Environment*, 1996, 30(30): 2981-2987.

1041 Seinfeld J H, Spyros N P. Atmospheric Chemistry and Physics: From Air Pollution to Clumate
1042 Change. John Wiley & Sons, 2016.

1043 Slemr, F., Angot, H., Dommergue, A., Magand, O., Barret, M., Weigelt, A., Ebinghaus, R.,
1044 Brunke, E. G., Pfaffhuber, K. A., Edwards, G., Howard, D., Powell, J., Keywood, M., and Wang,
1045 F.: Comparison of mercury concentrations measured at several sites in the Southern Hemisphere,
1046 Atmospheric Chemistry and Physics, 15, 3125-3133, 10.5194/acp-15-3125-2015, 2015.

1047 Sprovieri, F., Pirrone, N., Bencardino, M., amp, apos, Amore, F., Carbone, F., Cinnirella, S.,
1048 Mannarino, V., Landis, M., Ebinghaus, R., Weigelt, A., Brunke, E.-G., Labuschagne, C., Martin,
1049 L., Munthe, J., W ängberg, I., Artaxo, P., Morais, F., Barbosa, H. d. M. J., Brito, J., Cairns, W.,
1050 Barbante, C., Di éguéz, M. d. C., Garcia, P. E., Dommergue, A., Angot, H., Magand, O., Skov, H.,
1051 Horvat, M., Kotnik, J., Read, K. A., Neves, L. M., Gawlik, B. M., Sena, F., Mashyanov, N.,
1052 Obolkin, V., Wip, D., Feng, X. B., Zhang, H., Fu, X., Ramachandran, R., Cossa, D., Knoery, J.,
1053 Maruszczak, N., Nerentorp, M., and Norstrom, C.: Atmospheric mercury concentrations observed
1054 at ground-based monitoring sites globally distributed in the framework of the GMOS network,
1055 Atmospheric Chemistry and Physics, 16, 11915-11935, 10.5194/acp-16-11915-2016, 2016.

1056 Sprovieri, F., Pirrone, N., Bencardino, M., amp, apos, Amore, F., Angot, H., Barbante, C., Brunke,
1057 E.-G., Arcega-Cabrera, F., Cairns, W., Comero, S., Di éguéz, M. d. C., Dommergue, A., Ebinghaus,
1058 R., Feng, X. B., Fu, X., Garcia, P. E., Gawlik, B. M., Hagestr öm, U., Hansson, K., Horvat, M.,
1059 Kotnik, J., Labuschagne, C., Magand, O., Martin, L., Mashyanov, N., Mkololo, T., Munthe, J.,
1060 Obolkin, V., Ramirez Islas, M., Sena, F., Somerset, V., Spandow, P., Vard è M., Walters, C.,
1061 W ängberg, I., Weigelt, A., Yang, X., and Zhang, H.: Five-year records of mercury wet deposition
1062 flux at GMOS sites in the Northern and Southern hemispheres, Atmospheric Chemistry and
1063 Physics, 17, 2689-2708, 10.5194/acp-17-2689-2017, 2017.

1064 Sung, J.-H., Roy, D., Oh, J.-S., Back, S.-K., Jang, H.-N., Kim, S.-H., Seo, Y.-C., Kim, J.-H., Lee,
1065 C. B., and Han, Y.-J.: Trans-boundary movement of mercury in the Northeast Asian region
1066 predicted by CAMQ-Hg from anthropogenic emissions distribution, Atmospheric Research, 203,
1067 197-206, 10.1016/j.atmosres.2017.12.015, 2018.

1068 Wu, Q., Wang, S., Li, G., Liang, S., Lin, C. J., Wang, Y., Cai, S., Liu, K., and Hao, J.: Temporal
1069 Trend and Spatial Distribution of Speciated Atmospheric Mercury Emissions in China During
1070 1978-2014, Environ Sci Technol, 50, 13428-13435, 10.1021/acs.est.6b04308, 2016.

1071 Zhang, H., Fu, X. w., Lin, C. J., Shang, L. h., Zhang, Y. p., Feng, X. b., and Lin, C.: Monsoon-
1072 facilitated characteristics and transport of atmospheric
1073 mercury at a high-altitude background site in southwestern China, *Atmospheric Chemistry and*
1074 *Physics*, 16, 13131-13148, 10.5194/acp-16-13131-2016, 2016.

1075 Zhang, L., Wang, S. X., Wang, L., Wu, Y., Duan, L., Wu, Q. R., Wang, F. Y., Yang, M., Yang, H.,
1076 Hao, J. M., and Liu, X.: Updated emission inventories for speciated atmospheric mercury from
1077 anthropogenic sources in China, *Environ Sci Technol*, 49, 3185-3194, 10.1021/es504840m, 2015.

1078 Zhang, L., Wang, L., Wang, S., Dou, H., Li, J., Li, S., and Hao, J.: Characteristics and Sources of
1079 Speciated Atmospheric Mercury at a Coastal Site in the East China Sea Region, *Aerosol and Air*
1080 *Quality Research*, 17, 2913-2923, 10.4209/aaqr.2016.09.0402, 2017.

1081

1082 **Recent decrease trend of atmospheric mercury concentrations in East China: the**
1083 **influence of anthropogenic emissions**

1084 Yi Tang^{1,2}, Shuxiao Wang^{1,2*}, Qingru Wu^{1,2*}, Kaiyun Liu^{1,2}, Long Wang³, Shu Li¹, Wei Gao⁴, Lei
1085 Zhang⁵, Haotian Zheng^{1,2}, Zhijian Li¹, Jiming Hao^{1,2}

1086

1087 ¹ State Key Joint Laboratory of Environmental Simulation and Pollution Control, School of
1088 Environment, Tsinghua University, Beijing 100084, China

1089 ² State Environmental Protection Key Laboratory of Sources and Control of Air Pollution Complex,
1090 Beijing 100084, China

1091 ³ School of Environment and Energy, South China University of Technology, Guangzhou, 510006,
1092 China

1093 ⁴ Yangtze River Delta Center for Environmental Meteorology Prediction and Warning, Shanghai,
1094 20030, China

1095 ⁵ State Key Laboratory of Pollution Control & Resource Reuse, School of the Environment, Nanjing
1096 University, Nanjing, 210023, China

1097

1098

1099 * *Correspondence to:* Shuxiao Wang (shxwang@tsinghua.edu.cn)

1100 Qingru Wu (qrwu@tsinghua.edu.cn)

1101

1102 **Abstract**

1103 Measurements of gaseous elemental Hg (GEM), other air pollutants including SO₂, NO_x, O₃,
1104 PM_{2.5}, CO, and meteorological conditions were carried out at Chongming Island in East China from
1105 March 1 in 2014 to December 31 in 2016. During the sampling period, GEM concentrations
1106 significantly decreased from 2.68±1.07 ng m⁻³ in 2014 (March to December) to 1.60 ±0.56 ng m⁻³
1107 in 2016 (March to December). Monthly mean GEM concentrations showed a significant decrease
1108 with a rate of -0.60 ±0.08ng m⁻³ yr⁻¹ (R²=0.64, p<0.01 significance level). Combining the analysis
1109 of potential source contribution function (PSCF), principle component analysis (PCA), and
1110 emission inventory, we found that Yangtze River Delta (YRD) region was the dominant source
1111 region of GEM in Chongming Island and the main source industries included coal-fired power
1112 plants, coal-fired industrial boilers, and cement clinker production. We further quantified the effect
1113 of emission change on the air Hg concentration variations at Chongming Island through a coupled
1114 method of trajectory clusters and air Hg concentrations. It was found that the reduction of domestic
1115 emissions was the main driver of GEM decline in Chongming Island, accounting for 70% of the
1116 total decline. The results indicated that air pollution control policies targeting SO₂, NO_x and
1117 particulate matter reductions had significant co-benefits on GEM.

1118 **1 Introduction**

1119 Mercury (Hg) is of crucial concern to public health and the global environment for its
1120 neurotoxicity, long-distance transport, and bioaccumulation. The atmosphere is an important
1121 channel for global Hg transport. Once atmospheric Hg deposits to the aquatic system, it can be
1122 transformed into methylmercury (MeHg) which bio-accumulates through the food web and affects
1123 the central nervous system of human beings (Mason et al., 1995). Hg is therefore on the priority list
1124 of several international agreements and conventions dealing with environmental protection,
1125 including the *Minamata Convention on Mercury*.

1126 Atmospheric Hg exists in three operationally defined forms: gaseous elemental mercury (GEM),
1127 gaseous oxidized mercury (GOM), and particulate-bound mercury (PBM). And the sum of GEM
1128 and GOM is known as total gaseous mercury (TGM). In the atmosphere, Hg mainly presents as
1129 GEM, accounting for over 95% of the total in the most observation sites (Fu et al., 2015; Li et al.,
1130 2016; Zhang et al., 2017). GEM is stable and with low solubility in the troposphere with a long
1131 residence time and can be transported at regional and global scale (Lindberg et al., 2007). GEM can
1132 be oxidized through photochemical reaction to GOM, which can be converted to PBM upon
1133 adsorption/absorption on aerosol surfaces. GOM is much soluble than GEM, and PBM can be
1134 quickly scavenged by both dry and wet deposition. Therefore, the residence time of both GOM and
1135 PBM is shorter than that of GEM, generally several days to a few weeks for GOM and 0.5 – 2 year
1136 for GEM (Schroeder and Munthe, 1998).

1137 The atmospheric Hg observation results are important evidences to assess the effect of Hg
1138 emission control. During the past decades, significant decreases of GEM concentrations in Europe
1139 and North America have been observed (Cole et al., 2013; Weigelt et al., 2015). Air Hg
1140 concentrations in the northern hemisphere are reported to decline by 30-40% between 1990 and
1141 2010 (Zhang Y et al., 2016). Such a decrease is consistent with the decrease in anthropogenic Hg
1142 emissions inventory in Europe and North America (Streets et al., 2011). So far, most of the long-
1143 term observations on the ground sites have been carried out in the developed countries. For the
1144 developing countries such as China, limited atmospheric Hg observations have been carried out (Fu
1145 et al., 2008b; Zhang H et al., 2016; Hong et al., 2016) and there is no official national observing
1146 network of atmospheric Hg in mainland China. Therefore, there are few continuous multi-year

1147 observation records of China's air Hg concentrations published (Fu et al., 2015).
1148 China contributes to the largest Hg emissions in the world and will continue to be one significant
1149 Hg emitter for global Hg emissions in the coming future (UNEP, 2013, Wu et al., 2016, Chen et al.,
1150 2018; Pacyna et al., 2016). Large Hg emissions in China have led to the average air Hg
1151 concentrations of $2.86 \pm 0.95 \text{ ng m}^{-3}$ (in the range of 1.60-5.07 ng m^{-3}) at the remote sites in China
1152 (Fu et al., 2015). Such Hg concentration level is approximately 1.3 ng m^{-3} higher than the
1153 background concentration of GEM in Northern Hemisphere (Zhang et al., 2016; Sprovieri et al.,
1154 2017; Fu et al., 2015). In addition, the large Hg emissions in China will also impact the air Hg
1155 concentrations in East Asia and even North America through long-range transport (Sung et al.,
1156 2018; Zhang et al., 2017). Meanwhile, China has a great potential for Hg emission reduction during
1157 implementation of the *Minamata Convention on Mercury* (Chen et al., 2018). Therefore, long-term
1158 atmospheric Hg observations in China are critical to understand the Hg cycling at both regional and
1159 global scale. China's Hg emissions had increased from 147 t yr^{-1} in 1978 to around 538 t yr^{-1} in 2010
1160 due to the dramatic economic development (Zhang L et al., 2015; Wu et al., 2016; Hui et al., 2017).
1161 Atmospheric Hg monitoring that spanned the longest periods (from 2002 to 2010) in Guiyang,
1162 southwestern China witnessed the increase of Hg emissions in China (Fu et al., 2011). However,
1163 recently atmospheric Hg emissions in China have been estimated to decrease since 2012 (Wu et al.,
1164 2016). This decreasing trend needs to be confirmed by atmospheric Hg observations.

1165 In this study, we measured GEM, other air pollutants (eg., $\text{PM}_{2.5}$ and NO_x), and meteorological
1166 parameters (eg., temperature and wind speed) at a remote marine site of Chongming Island in East
1167 China during 2014-2016. We analyzed annual and seasonal variation of GEM and the potential
1168 impact factors. Combining the analysis of potential source contribution function (PSCF), principle
1169 component analysis (PCA), and emission inventory, the potential source regions and source
1170 industries of atmospheric Hg pollution at the monitoring site are identified. In addition, a coupled
1171 trajectories and air Hg concentration method is developed to assess the effect of Hg emission change
1172 from different regions on air GEM concentration variation at the monitoring site.

1173 **2 Materials and methods**

1174 **2.1 Site descriptions**

1175 The monitoring remote site (31°32'13"N, 121°58'04"E, about 10 m above sea level) locates at the
1176 top of weather station in Dongtan Birds National Natural Reserve, Chongming Island, China (Figure
1177 1). As China's third largest island, Chongming Island is located in the east of Yangtze River Delta
1178 region with a typical subtropical monsoon climate. It is rainy, hot, with southern and southeastern
1179 winds in summer and is dry, cold, and with northwestern wind in winter. The dominant surface types
1180 are farmland and wetland. There are no large anthropogenic emission sources in the island and no
1181 habitants within 5 km distance from the site. The downtown Shanghai area is 50 km to the southwest
1182 of the site.

1183 **2.2 Sampling methods and analysis**

1184 During the monitoring period, we used Tekran 2537X/1130/1135 instruments to monitor
1185 speciated Hg in the atmosphere, which was widely used for air Hg observation in the world. The
1186 sampling inlet was 1.5 m above the instrument platform. Continuous 5-minute of GEM was
1187 measured by Tekran 2537X Hg vapor analyzer with the detection limit of 0.1 ng m⁻³ at a sampling
1188 flow rate of 1.0 L min⁻¹ during two campaigns: March 1, 2014 to December 31, 2015 and March 26
1189 to December 31, 2016. From July 5, 2015 to April 30 2016, the Tekran 1130/1135 speciation unit
1190 was damaged by the rainstorm, the Tekran 2537X were operated without speciation units but with
1191 PTFE filter to protect the instrument from particles and sea salt. Therefore, the observed
1192 concentrations during July 2015-April 2016 were TGM concentrations indeed. However, the GOM
1193 concentrations at Chongming Island accounted for less than 1% of TGM (TGM=GOM+GEM).
1194 Thus, the GEM concentrations were approximated to TGM concentrations from July 2015 to April
1195 2016.

1196 The 2537X analyzer was calibrated automatically every 25 h using the internal Hg permeation
1197 source inside the instrument, and the internal permeation source was calibrated every 12 months
1198 with manual injection of Hg by a syringe from an external Hg source (module 2505). Two zero and
1199 two span calibrations were performed for each calibration of gold trap A and B, respectively. The
1200 difference between gold trap A and gold trap B was limited to ±10%. The impactor plates and quartz
1201 filter were changed in every two weeks. The soda lime was changed once a month. The denuders

1202 were recoated once every two weeks following the procedure developed by Landis et al. (2002).

1203 In our research, random uncertainties of individual measurement had been averaged out and the
1204 systematic uncertainties need to be considered. The overall practically achievable systematic
1205 uncertainty would be 10% considering that the instrument was not in ideal performance (Slemr et
1206 al., 2015; Steffen et al., 2012). For example, slow deactivation of the traps, contamination of the
1207 switching valves and leaks would increase the uncertainties but were difficult to quantify (Slemr et
1208 al., 2015; Steffen et al., 2012). Because of the consistency of instrument and the quality
1209 assurance/quality control have been paid special attention to during the sampling campaign, the
1210 systematic differences of instrument did not affect the huge variation between 2014 and 2016.

1211 During the sampling campaigns, PM_{2.5}, O₃, NO_x, CO and SO₂ were also monitored by Thermo
1212 Scientific TEOM 1405D, Model 49i O₃ Analyzer, Model 48i CO Analyzer, Model 42i-TL NO_x
1213 Analyzer and Model 43i SO₂ Analyzer, respectively. The detection limits of O₃, SO₂, NO_x, CO and
1214 PM_{2.5} are 1.0, 0.5, 0.4, 0.04 and 0.1 µg m⁻³, respectively. The meteorological parameters including
1215 air temperature, wind speed, and wind direction are measured by Vantage Pro2 weather station
1216 (Davis Instruments). The instruments are tested and calibrated periodically. All data are hourly
1217 averaged in this study.

1218 **2.3 Sources apportionment of atmospheric Hg pollution**

1219 2.3.1 PSCF model

1220 To identify the source areas for pollutants with a relatively long lifetime such as GEM (Xu and
1221 Akhtar, 2010), the PSCF values for mean GEM concentrations in grid cells in a study domain are
1222 calculated by counting the trajectory segment endpoints that terminate within each cell. The number
1223 of endpoints that fall in the *ij*-th cell are designated *n_{ij}*. The number of endpoints for the same cell
1224 having arrival times at the monitoring site corresponding to GEM concentrations higher than a
1225 specific criterion is defined to be *m_{ij}*. The criterion in this study is set as the average Hg concentration
1226 during our study period. The PSCF value for the *ij*-th cell is then defined as:

$$1227 \quad PSCF_{ij} = \frac{m_{ij}}{n_{ij}} W_{ij} \quad (1)$$

1228 where *W_{ij}* is an empirical weight to reduce the effects of grid cells with small *n_{ij}* values. In this
1229 study, *W_{ij}* is defined as in the following formula, in which *Avg* is the mean *n_{ij}* of all grid cells with
1230 *n_{ij}* greater than zero:

$$W_{ij} = \begin{cases} 1.0 & n_{ij} > 2 * Avg \\ 0.7 & Avg < n_{ij} \leq 2 * Avg \\ 0.42 & 0.5 * Avg < n_{ij} \leq Avg \\ 0.17 & n_{ij} \leq 0.5 * Avg \end{cases} \quad (2)$$

1232 The PSCF value indicates the probability of a grid cell through which polluted events occurs.
 1233 More method details can be found in the study of Polissar et al. (Polissar et al., 1999). In this study,
 1234 the domain that covered the potential contribution source region (105 °–135 °E, 15 °–45 °N) was
 1235 divided into 22500 grid cells with 0.2 °×0.2 ° resolution. 72-hour back trajectories were generated
 1236 hourly from 1 March, 2014 to 31 December, 2015 and from March 26 to December 31 in 2016 by
 1237 TrajStat, a software including HYSPLIT for trajectory calculation with trajectory statistics modules
 1238 (Wang et al., 2009). PSCF map was plotted using ArcGIS version 10.1.

1239 2.3.2 Principal component analysis (PCA)

1240 Correlation between Hg and other pollutant concentrations are used to identify source industries.
 1241 Strong positive loadings (loading>0.40) with SO₂ and PM_{2.5} typically indicate the impact of coal
 1242 combustion, and strong positive loadings with GEM and CO have often been used as an indicator
 1243 for regional transport because both pollutants have similar source and stable chemical properties
 1244 (Lin et al., 2006; Pirrone et al., 1996). In this study, PCA was applied to infer the possible influencing
 1245 factors of GEM in 2014 and 2016. Prior to analysis, each variable was normalized by dividing its
 1246 mean, and pollutant concentrations (SO₂, CO, NO_x, PM_{2.5}) were averaged to 1-h sampling intervals
 1247 to match the hourly Hg monitoring during sampling period. The results in 2016 had no CO data due
 1248 to instrument broken. Statistics analyses were carried out by using SPSS 19.0 software.

1249 **2.4 Quantification method of source contribution**

1250 To further quantitatively assess the effect of change in emissions from different regions on air
 1251 concentrations variation at a certain monitoring site, a quantitative estimation method which coupled
 1252 trajectories with air Hg concentrations was developed. We firstly identified the trajectories by using
 1253 the National Oceanic and Atmospheric Administration (NOAA) Hybrid Single-Particle Lagrangian
 1254 Integrated Trajectory (HYSPLIT) model. The gridded meteorological data at a horizontal resolution
 1255 of 1 °×1 ° were obtained from the Global Data Assimilation System (GDAS) (Draxler and Hess,
 1256 1998). The starting heights were set to be 500 m above ground level to represent the center height
 1257 of boundary layer where pollutants are usually well mixed in boundary layer. Secondly, each
 1258 trajectory was assigned with GEM concentration by matching the arriving time in Chongming site.

1259 Third, the backward trajectories which coupled with Hg concentrations were clustered into groups
 1260 according to transport patterns by using NOAA HYSPLIT 4.7. Thus, the grouped clusters were
 1261 applied to identify the Hg source regions. The Hg average concentration of the cluster j was then
 1262 calculated as equation (3). And, the trajectory weighted concentration in the cluster j as equation
 1263 (4). At last, the contribution of reduction at a certain region on Hg concentration at monitoring sites
 1264 in a certain period can be calculated as equation (5).

1265

$$1266 \quad C_{j,t} = \frac{\sum_{i=1}^n C_{i,j,t}}{\sum_{i=1}^n N_{i,j,t}} \quad (3)$$

$$1267 \quad TWC_{j,t} = AR \times C_{j,t} \quad (4)$$

1268 where N refers to a certain trajectory. j refers to a certain cluster. t is the studied period, and n is
 1269 the number of trajectory. m is the number of cluster. C is the GEM concentration, ng m^{-3} . TWC refers
 1270 to the trajectory weighted concentration, ng m^{-3} . In order to reduce the influence of trajectory
 1271 changes in different region between calculated years, the average ratio (AR) was used here for
 1272 calculating TWC.

$$1273 \quad CR_j = \frac{TWC_{j,t_2} - TWC_{j,t_1}}{\sum_{j=1}^m TWC_{j,t_2} - \sum_{j=1}^m TWC_{j,t_1}} \quad (5)$$

1274 where CR refers to the contribution of GEM reduction. t_1 and t_2 refers to the two period
 1275 participating to comparison, namely year 2014 and 2016 in this study, respectively.

1276 This approach is a simple method to quantify the influence of anthropogenic emissions on GEM
 1277 concentration variation. It should be noted that uncertainties always exist in calculating trajectories,
 1278 causing uncertainties in all trajectory-based approaches. Trajectory errors vary considerably in
 1279 different situation. Draxler (1996) suggested uncertainties might be 10% of the travel distance.
 1280 Besides, meteorological conditions were pretty similar in 2014 and 2016 so as to reduce the
 1281 interference from meteorology (Table S2).

1282 2.5 Regional atmospheric Hg emissions

1283 Regional anthropogenic GEM emissions by month are calculated by using both the technology-

1284 based emission factor methods and transformed normal distribution function method. Detailed
1285 introduction of these two methods and the speciation profile of the emitted Hg for each sector are
1286 described in our previous study (Wu et al., 2016). Conventional air pollutant (SO₂, PM_{2.5}, and NO_x)
1287 emissions were calculated following the study of Zhao et al. (2013). The source regions included in
1288 the emission inventory consisted of Shanghai, Jiangsu, Zhejiang, and Anhui provinces according to
1289 the PSCF results (See section 3.3). The studied emission sectors included coal-fired power plants,
1290 coal-fired industrial boilers, residential coal-combustion, cement clinker production, iron and steel
1291 production, mobile oil combustion and other small emission sectors (eg., zinc smelting, lead
1292 smelting, municipal solid incineration, copper smelting, aluminum production, gold production,
1293 other coal combustion, stationary oil combustion, and cremation). The monthly Hg emissions were
1294 mainly distributed according to fuel combustions or products productions by month (Table S1). For
1295 small emission sectors, the annual emissions were equally distributed into monthly emissions. The
1296 GEM emissions from natural sources E_N are calculated as followings.

1297
$$E_N = \sum_i F_i \times A_i \times t \quad (6)$$

1298 where F_i is a bi-directional Hg flux of canopy i , ng km⁻² yr⁻¹; A is the studied area, km²; t is the
1299 studied year, yr. The bi-directional Hg flux was obtained from the study of Wang et al. (2016)
1300 directly. It should be pointed out that the natural emission is a concept of net emission in this
1301 manuscript, which reflected a net effect of two competing processes (Zhang, 2009): total Hg natural
1302 emissions and total Hg deposition. The total natural emissions included primary natural release and
1303 re-emission of legacy Hg stored in the terrestrial and water surface (Wang et al., 2016). When the
1304 value is positive, it means the net effect is Hg emissions to air. Otherwise, Hg deposited.

1305 **3 Results and discussions**

1306 **3.1 Decreasing trends of atmospheric Hg during 2014-2016**

1307 The average concentrations of GEM in 2014 (March to December), 2015 and 2016 (March to
1308 December) were 2.68 ± 1.07 ng m⁻³, 2.14 ± 0.82 ng m⁻³, and 1.60 ± 0.56 ng m⁻³, respectively. The
1309 GEM concentrations in 2014 were higher (t test, $p < 0.01$) than the Northern Hemisphere back-
1310 ground concentration (about 1.5 ng m⁻³) (Sprovieri et al., 2010) and those measured in other remote
1311 and rural locations in China (Zhang H et al., 2015; Fu et al., 2008a; Fu et al., 2009). However, in

1312 2016, the GEM concentrations were similar to the background concentrations in the Northern
1313 Hemisphere. During this period, monthly GEM concentrations showed a significant decrease with
1314 a rate of $-0.60 \pm 0.08 \text{ ng m}^{-3} \text{ yr}^{-1}$ ($R^2=0.64$, $p<0.01$ significance level, $n = 32$) (Figure 2a). The
1315 amount of valid data for each month was shown in Table S3. From another aspect, the trend
1316 decomposition of the GEM concentration signal (signal = trend + seasonal + random) from March
1317 2014 to December 2016 were performed in Figure 2 ([https://anomaly.io/seasonal-trend-](https://anomaly.io/seasonal-trend-decomposition-in-r/)
1318 [decomposition-in-r/](https://anomaly.io/seasonal-trend-decomposition-in-r/)). By using this method, we also observed a pronounced trend (Figure 2b) and
1319 the random was limited in the range of $-0.24 - 0.24 \text{ ng m}^{-3}$ (Figure 2d).

1320 One potential worry is that the calculated trend will be sensitive to seasonal variation and the
1321 missing data in January and February of 2016 may impact the downward trend. To evaluate the
1322 impact of the missing data, we estimate the Hg concentrations in the missing months based on the
1323 data of the same months in 2015 and 2017 (Figure S1). Combining the estimated data, we re-fit the
1324 Hg concentrations and downward trend still maintained robust and similar to the downward trend
1325 in manuscript (Figure S1). Thus, we assume that the missing data is not very important and will not
1326 impact our main conclusion.

1327 Table S4 showed the Hg variation trends in different regions. Significant decreases of GEM
1328 concentrations in North hemisphere over the past two decades have been well documented (Weigelt
1329 et al., 2015; Cole et al., 2013; Kim et al., 2016). All the stations in Table S4 used Tekran instruments
1330 except for the observation in South Korea. Different instruments could cause potential differences
1331 in the observation, but they were comparable and did not affect the conclusion of comparison in
1332 downward trend (Slemr et al., 2015; Sprovieri et al., 2016). Weigelt et al. (2015) showed that GEM
1333 concentrations decreased from 1.75 ng m^{-3} in 1996 to 1.4 ng m^{-3} in 2009 at Mace Head, Europe.
1334 Ten-year trends of GEM concentrations at six ground-based sites in the Arctic and Canada also
1335 showed a decreasing trend at a rate of $13\text{-}35 \text{ pg m}^{-3} \text{ y}^{-1}$ (Cole et al., 2013). In South Korea, the
1336 observed GEM concentration also had significant decrease in recent years (Kim et al., 2016). In
1337 South Africa, annual average GEM concentration at Cape Point decreased from 1.29 ng m^{-3} in
1338 1996 to 1.19 ng m^{-3} in 2004 (Slemr et al., 2008) and were increasing from 0.93 ng m^{-3} in 2007
1339 (Slemr et al., 2015) until 2016 (Martin et al, 2017). However, limited GEM monitoring sites and
1340 relative short-time spans in China restricted the views of long-term trends in atmospheric Hg
1341 concentration in this region. A preliminary assessment indicated that atmospheric Hg concentrations

1342 in China kept increasing before 2012 (Fu et al., 2015). The decreasing trend observed in our study
1343 was accordant with reported data in Mt. Changbai during 2014-2015 cited in the review of Fu et al.
1344 (2015). The atmospheric Hg at Chongming was influenced by and in turn reflected regional Hg
1345 emission and cycle. Although the decline in atmospheric Hg was observed in many sites of the
1346 Northern Hemisphere, much sharper decrease of Hg concentrations was observed at Chongming in
1347 our study. The specific reasons for the Hg concentration decrease in our study will be discussed in
1348 section 3.4.

1349 **3.2 Seasonal variation of GEM concentrations**

1350 According to the decomposition result (Figure 2c), we observed strong seasonal cycle at
1351 Chongming. The GEM concentrations were highest in July and lowest in September, so GEM
1352 concentrations in the same month from different years were averaged to understand the
1353 detrended seasonal circle (Figure 3). The error bars in the Figure 3 meant the standard deviation
1354 of the monthly average. Observed GEM concentrations showed an obvious seasonal cycle. The
1355 mean GEM concentration in warm season (from April to September) is 0.29 ng m^{-3} higher than that
1356 in cold season. Such seasonal variation trend is also observed at Nanjing, Miyun, Mt. Ailao, Mt.
1357 Waliguan, and Shangri-La (Zhang et al., 2013; Zhang et al., 2016; Fu et al., 2015; Zhu et al., 2012).
1358 On the other hand, the means of GEM at Mt. Gongga, Mt. Daimei, Mt. Leigong, and Mt. Changbai
1359 in China are relatively higher in cold seasons. The average of atmospheric Hg concentrations in the
1360 north hemisphere also have a trough value in summer (Sprovieri et al., 2016).

1361 Seasonal variations of GEM concentration are generally attributed to the following factors,
1362 including natural and anthropogenic emissions, atmospheric chemical reaction, and air mass
1363 transportation. The higher Hg concentrations in cold seasons in Mt. Leigong were mainly
1364 explained by coal-combustion for urban and residential heating during cold seasons. Whereas,
1365 increasing solar radiation and soil/air temperature dominate the higher Hg concentrations in Mt.
1366 Ailao. In addition, sites in southern, eastern, and northeastern China also impacted from
1367 anthropogenic emissions of GEM from the north and west by the northerly winter monsoon while
1368 the sites located in western, southwestern, and northern China were impacted in the warm season
1369 (Fu et al., 2015). As to most sites in the northern hemisphere, high wet Hg precipitation induced
1370 probably by faster GEM oxidation led to lower Hg concentrations in summer.

1371 Source emission is one significant factor on GEM concentrations in the air. The GEM

1372 concentrations at a remote site are generally regarded under the impact of regional emissions.
1373 Therefore, the emissions in the YRD regions (Anhui, Zhejiang, Jiangsu, and Shanghai) were
1374 calculated. However, the anthropogenic emissions were in the range of 2.5-2.7 t, which is almost
1375 unchanged. Compared to the anthropogenic emissions, we observed almost synchronized trends
1376 between natural emissions and air Hg concentrations in Figure 4. The natural emissions showed a
1377 huge seasonal variation, from -5.4 t to 8.4 t. The largest natural emissions were observed in summer
1378 when the highest GEM concentrations were monitored. In the autumn, the natural emissions
1379 performed as the largest deposition direction amount and the GEM concentrations were the lowest
1380 in the whole year. Therefore, natural emissions instead of anthropogenic were supposed to be one
1381 significant factor of the seasonal cycle of GEM concentrations (Figure 4). The seasonal trend of
1382 natural emissions is closely related with the canopy types in YRD areas, where widely subtropical
1383 forests, paddy field, and dry farming were observed (Figure S2). The high temperature will speed
1384 up decomposition of organic compound in soil, which leads to Hg emissions from farmland and
1385 forest in YRD region (Luo et al., 2016; Yu et al., 2017). In autumn and winter, with the decrease of
1386 temperature (Table S2), the role of soil changed from Hg source to sink, which reduces the Hg
1387 concentrations in the air (Wang et al., 2016). At the same time, the growing vegetation in autumn
1388 also absorbs air Hg, resulting lower Hg concentrations compared to that in winter. Transport also
1389 overall enhanced the observed seasonal variation of GEM concentrations at Chongming Island.
1390 According to the statistics of backward trajectories in section 3.4, the GEM concentrations in the
1391 air mass which did not pass via the YRD regions also showed high GEM concentration in warm
1392 season in 2014 (Figure S3).

1393 From Figure 2, we also observed more pronounced seasonal variation in 2014, which can be
1394 attributed to the lower wet deposition and GEM oxidation. On one aspect, as a costal site, the
1395 Chongming Island is abundant with •OH. The increase of O₃ concentration from the summer of
1396 2014 to 2016 may contribute to a higher oxidation of GEM in 2016. On another aspect, higher wet
1397 Hg deposition in summer is approximately 6.6 times of that in the winter at Chongming (Zhang et
1398 al., 2010). Meanwhile, the rainfall in 2016 summer (546 mm) was higher than the rainfall in 2014
1399 (426 mm). Therefore, the higher oxidation and wet deposition rate of Hg in the summer of 2016
1400 will reduce the concentration difference between summer and winter, which lead to a less
1401 pronounced seasonal variation in 2016. Meanwhile, the higher oxidation and wet deposition in

1402 2016 also contributed to the downward trend of GEM by reducing the seasonality in spring and
1403 summer (Figure S3).

1404 3.3 Source apportionment of atmospheric Hg pollutions

1405 According to the PSCF result, YRD region, including Shanghai, Jiangsu, Anhui, and Zhejiang
1406 provinces, was the dominant source region in both 2014 and 2016 (Figure 5). Therefore, Hg
1407 emissions from these areas would contribute to high proportion of Hg pollution at Chongming Island.
1408 The offshore area mainly around Jiangsu province also has a high PSCF value because some
1409 trajectories from North China, especially Shandong province, transport to Chongming Island
1410 through this area. Compared to the result in 2014, the PSCF value had an obvious decline in East
1411 China Sea in 2016. The decline from the East China Sea may be contributed by the downward trend
1412 of GEM concentrations in South Korea and Japan (Kim et al., 2016; Kim et al., 2013), where the
1413 anthropogenic Hg emissions of Japan and South Korea have been reduced by 13% and 4% during
1414 2010-2015, respectively (UNEP 2013; UNEP 2018). The air mass from Japan and South Korea
1415 would pass through the East China Sea to Chongming.

1416 PCA method was applied to preliminarily identify the source industries. In the studied period,
1417 totally 2 factors were identified in 2014 and 2016, respectively. The factor 1 had strong factor
1418 loadings of GEM, SO₂, NO_x, CO, and PM_{2.5} in both 2014 and 2016 (No CO data in 2016 due to
1419 equipment problems). The factor 1 accounted for 49% variance in 2014 and 50% variance in 2016
1420 (Table 1). The results indicated common significant source sectors of the above five air pollutants,
1421 which can also be proven from emission inventories (Table 2). The dominant source industries
1422 included coal-fired power plants, coal-fired industrial boilers, and cement clinker production. The
1423 PCA results showed that anthropogenic emissions were the main sources of GEM during the
1424 sampling period.

1425 The factor 2 in both 2014 and 2016 had a strong positive loading on O₃ and negative loading on
1426 NO_x. Considering the low loading of CO and high loading of O₃, the factor 2 can be viewed as a
1427 sign of the transport of air mass from stratosphere (Fishman and Seiler, 1983; Jaffe, 2010). The air
1428 mass from stratosphere will increase the O₃ concentration. O₃ react with NO, which makes a
1429 negative correlation with NO. However, the low loading on GEM of factor 2 indicated that Factor
1430 2 had no relationship with GEM concentrations at Chongming from the aspect of whole year data.

1431 **3.4 The influence of anthropogenic emissions**

1432 To further understand the reason of the downward trend, we firstly compared the meteorological
1433 conditions in both 2014 and 2016. We noted that the difference of annual temperature, solar radiation,
1434 and relative humidity were constrained in the range of 17.13 ± 7.48 °C, 165.55 ± 45.87 W m⁻² and
1435 $75.38\pm 5.82\%$, respectively (Table S2). The coefficient of variation for annual mean of these
1436 meteorological conditions in 2014 and 2016 was 2.6%, 6.7% and 0.2%, respectively. In addition,
1437 the wind rose was similar, and the dominating wind was from SE in both 2014 and 2016 (Figure
1438 S4). The HYSPLIT results also provided similar trajectories in 2014 and 2016 (Figure 6). Therefore,
1439 we assumed that the meteorological condition was not the dominant reason of GEM decline at
1440 Chongming site.

1441 To further quantify the driver of GEM decline, a trajectory-based analysis method was used in
1442 this study. The 72-h air mass back trajectories were calculated using HYSPLIT for every 8 hours
1443 starting at the observation site. Approximately 918 and 832 trajectories were calculated in sampling
1444 period in 2014 (Mar 1 to Dec 31, 2014) and 2016 (Mar 26 to Dec 31, 2016), respectively. The
1445 trajectories were grouped into 3 clusters in each year according to geographical regions (Figure 6).
1446 The first cluster of trajectories mainly passed through the regions (eg., North China) north and
1447 northwest to Chongming Island before arriving to our monitoring site, which was denoted as cluster
1448 NCP. The second cluster mainly passed YRD region to Chongming, which was signed as cluster
1449 SW-YRD. The third type mainly originated from the East China Seas, South Korea, Japan and
1450 Northeast Asia continent, and then arrived to our monitoring sites directly without passing the
1451 mainland China. This type of trajectories was named as cluster ABROAD. Some trajectories
1452 originated from the East China Sea and crossed the mainland China before arriving Chongming
1453 were grouped into cluster NCP or SW-YRD depending on the regions it crossed. The trajectories
1454 for each of the three clusters in 2014 and 2016 were shown in Table 3.

1455 Table 3 showed the detail statistics data of the three classifications. From 2014 to 2016, the whole
1456 China region (NCP, SW-YRD) contributed to 70% of GEM decline at Chongming Island.
1457 Considering downward trend of emission inventory and atmospheric pollutant from 2014 to 2016
1458 in NCP and SW-YRD region (Table S5, Table S6), the reason of downward trend can be attributed
1459 to the effectiveness of existing air pollution control measures in China (SC, 2013; MEP, 2014).
1460 Meanwhile, the cluster NCP, cluster SW-YRD, and cluster ABROAD caused 26%, 44%, and 30%

1461 for GEM decline, respectively (Table 3). The cluster SW-YRD contributed to 44% of reduction,
1462 suggesting that air pollution controls on anthropogenic emissions in YRD region dominated the
1463 recent decrease of GEM concentrations at Chongming site. The largest decline of Hg concentration
1464 (1.32 ng m^{-3}) was also observed in the cluster SW-YRD demonstrated the efficiency of emission
1465 reduction in YRD region (Table S5, Table S6). Moreover, ABROAD region caused 30% of GEM
1466 decline from 2014 to 2016, which implies global effort on atmospheric Hg emission control under
1467 the guidance of *Minamata Convention on Mercury*.

1468 **4 Conclusion**

1469 Atmospheric Hg was continuously measured for three years at a regional background site in the
1470 YRD region. During the sampling period, a downward trend for GEM concentrations (-0.60 ± 0.08
1471 $\text{ng m}^{-3} \text{ y}^{-1}$) at Chongming Island was observed. The seasonal GEM cycle was dominated by the
1472 natural emissions while the annual GEM concentration trend was mainly impacted by anthropogenic
1473 emissions. By using a new approach that considers both cluster frequency and the Hg concentration
1474 associated with each cluster, we quantified that atmospheric Hg from NCP region, SW-YRD region,
1475 and ABROAD region have caused 26%, 44%, and 30% decline of GEM concentrations at
1476 Chongming monitoring site, respectively. The result suggested that reduction of anthropogenic
1477 emissions in mainland China was the main cause of the recent decreasing trend of GEM
1478 concentration at Chongming site. The air pollution control policies in China, especially the pollution
1479 control in the coal-fired power plants, coal-fired industrial boilers, and cement clinker production
1480 in YRD region and Shandong province, have received significant co-benefit of atmospheric Hg
1481 emission reductions. On the other hand, emission reduction from the ABROAD region, where
1482 clusters arrived to Chongming monitoring site directly without passing the mainland China, implies
1483 global effort on atmospheric Hg emission control under the guidance of *Minamata Convention on*
1484 *Mercury*. Considering that the *Minamata Convention on Mercury* had come into force in 2017,
1485 continuous long-term observation of atmospheric Hg in China will be required for the assessment
1486 of policy effectiveness.

1487

1488 *Data availability.* All data are available from the authors upon request.

1489

1490 *Competing interests.* The authors declare that they have no conflict of interest.

1491

1492 *Acknowledge.* This work is sponsored by the Natural Science Foundation of China (No. 21607090),

1493 Major State Basic Research Development Program of China (973 Program) (No. 2013CB430000),

1494 National Key R&D Program of China (No. 2016YFC0201900)

1495

1496

1497

1498

1499

1500 **References**

- 1501 Cole, A. S., Steffen, A., Pfaffhuber, K. A., Berg, T., Pilote, M., Poissant, L., Tordon, R., and Hung,
1502 H.: Ten-year trends of atmospheric mercury in the high Arctic compared to Canadian sub-Arctic
1503 and mid-latitude sites, *Atmospheric Chemistry and Physics*, 13, 1535-1545, 2013.
- 1504 Chen, L., Zhang, W., Zhang, Y., Tong, Y., Liu, M., Wang, H., Xie, H., and Wang, X.: Historical and
1505 future trends in global source-receptor relationships of mercury, *Science of the Total Environment*,
1506 610-611, 24-31, 2018.
- 1507 Draxler, R. R.: Trajectory Optimization for Balloon Flight Planning, *International Journal for*
1508 *Numerical Methods in Fluids*, 5, 13-23, 1996.
- 1509 Draxler, R. R., and Hess, G. D.: An overview of the hysplit-4 modeling system for trajectories,
1510 *Australian Meteorological Magazine*, 47, 295-308, 1998.
- 1511 Fishman J, Seiler W. Correlative Nature of Ozone and Carbon Monoxide in the Troposphere:
1512 Implications for the Tropospheric Ozone Budget. *Journal of Geophysical Research*, 88(C6), 1983.
- 1513 Fu, X. W., Feng, X. B., Zhu, W. Z., Wang, S. F., and Lu, J. L.: Total gaseous mercury concentrations
1514 in ambient air in the eastern slope of Mt. Gongga, South-Eastern fringe of the Tibetan plateau, China,
1515 *Atmospheric Environment*, 42, 970-979, 2008a.
- 1516 Fu, X. W., Feng, X. B., Zhu, W. Z., Zheng, W., Wang, S. F., and Lu, J. Y.: Total particulate and
1517 reactive gaseous mercury in ambient air on the eastern slope of the Mt. Gongga area, China, *Applied*
1518 *Geochemistry*, 23, 408-418, 2008b.
- 1519 Fu, X. W., Feng, X. B., Wang, S., Rothenberg, S., Shang, L., Li, Z., and Qiu, G.: Temporal and
1520 spatial distributions of total gaseous mercury concentrations in ambient air in a mountainous area
1521 in southwestern China: implications for industrial and domestic mercury emissions in remote areas
1522 in China, *Science of the Total Environment*, 407, 2306-2314, 2009.
- 1523 Fu, X. W., Feng, X. B., Qiu, G. L., Shang, L. H., and Zhang, H.: Speciated atmospheric mercury
1524 and its potential source in Guiyang, China, *Atmospheric Environment*, 45, 4205-4212, 2011.
- 1525 Fu, X. W., Zhang, H., Yu, B., Wang, X., Lin, C. J., and Feng, X. B.: Observations of atmospheric
1526 mercury in China: a critical review, *Atmospheric Chemistry and Physics*, 15, 9455-9476, 2015.
- 1527 Hong, Q. Q., Xie, Z. Q., Liu, C., Wang, F. Y., Xie, P. H., Kang, H., Xu, J., Wang, J. C., Wu, F. C.,
1528 He, P. Z., Mou, F. S., Fan, S. D., Dong, Y. S., Zhan, H. C., Yu, X. W., Chi, X. Y., and Liu, J. G.:

1529 Speciated atmospheric mercury on haze and non-haze days in an inland city in China, *Atmospheric*
1530 *Chemistry and Physics*, 16, 13807-13821, 2016.

1531 Hui, M. L., Wu, Q. R., Wang, S. X., Liang, S., Zhang, L., Wang, F. Y., Lenzen, M., Wang, Y. F., Xu,
1532 L. X., Lin, Z. T., Yang, H., Lin, Y., Larssen, T., Xu, M., and Hao, J. M.: Mercury flows in China and
1533 global drivers, *Environmental Science & Technology*, 51, 222-231, 2017.

1534 Jaffe, D.: Relationship between surface and free tropospheric ozone in the western U.S.,
1535 *Environmental Science & Technology*, 45, 432-438, 2010.

1536 Kim, K.-H., Yoon, H.-O., Brown, R. J. C., Jeon, E.-C., Sohn, J.-R., Jung, K., Park, C.-G., and Kim,
1537 I.-S.: Simultaneous monitoring of total gaseous mercury at four urban monitoring stations in Seoul,
1538 Korea, *Atmospheric Research*, 132-133, 199-208, 2013.

1539 Kim, K. H., Brown, R. J. C., Kwon, E., Kim, I. S., and Sohn, J. R.: Atmospheric mercury at an urban
1540 station in Korea across three decades, *Atmospheric Environment*, 131, 124-132, 2016.

1541 Landis, M. S., Stevens, R. K., Schaedlich, F., and Prestbo, E. M.: Development and characterization
1542 of an annular denuder methodology for the measurement of divalent inorganic reactive gaseous
1543 mercury in ambient air, *Environmental Science & Technology*, 36, 3000-3009, 2002.

1544 Lindberg, S., Bullock, R., Ebinghaus, R., Engstrom, D., Feng, X. B., Fitzgerald, W., Pirrone, N.,
1545 Prestbo, E., and Seigneur, C.: A synthesis of progress and uncertainties in attributing the sources of
1546 mercury in deposition, *Ambio*, 36, 19, 2007.

1547 Li, S., Gao, W., Wang, S. X., Zhang, L., Li, Z. J., Wang, L., and Hao, J. M.: Characteristics of
1548 Speciated Atmospheric Mercury in Chongming Island, Shanghai, *Environmental Science* 37, 3290
1549 - 3299, 2016.

1550 Luo, Y., Duan, L., Driscoll, C. T., Xu, G., Shao, M., Taylor, M., Wang, S. X., and Hao, J. M.:
1551 Foliage/atmosphere exchange of mercury in a subtropical coniferous forest in south China, *Journal*
1552 *of Geophysical Research Biogeosciences*, 121, 2016.

1553 Martin, L. G., Labuschagne, C., Brunke, E. G., Weigelt, A., Ebinghaus, R., and Slemr, F.: Trend of
1554 atmospheric mercury concentrations at Cape Point for 1995–2004 and since 2007, *Atmospheric*
1555 *Chemistry and Physics*, 17, 2393-2399, 2017.

1556 Mason, R. P., Reinfelder, J. R., and Morel, F. M. M.: Bioaccumulation of mercury and
1557 methylmercury, Springer Netherlands, 915-921 pp., 1995.

1558 Ministry of Environmental Protection (MEP) and State Administration for Quality Supervision and

1559 Inspection and Quarantine (AQSIQ): Emission standard of air pollutants for boilers, MEP, Beijing,
1560 China, 2014.

1561 Pirrone, N., Keeler, G. J., and Nriagu, J. O.: Regional differences in worldwide emissions of mercury
1562 to the atmosphere, *Atmospheric Environment*, 30, 2981-2987, 1996.

1563 Polissar, A. V., Hopke, P. K., Paatero, P., Kaufmann, Y. J., Hall, D. K., Bodhaine, B. A., Dutton, E.
1564 G., and Harris, J. M.: The aerosol at Barrow, Alaska: long-term trends and source locations,
1565 *Atmospheric Environment*, 33, 2441-2458, 1999.

1566 State Council of the People's Republic of China (SC): Action plan of national air pollution
1567 prevention and control, SC, Beijing, China, 2013.

1568 Schroeder, W. H., and Munthe, J.: Atmospheric mercury—An overview, *Atmospheric Environment*,
1569 32, 809-822, 1998.

1570 Slemr, F., Angot, H., Dommergue, A., Magand, O., Barret, M., Weigelt, A., Ebinghaus, R., Brunke,
1571 E. G., Pfaffhuber, K. A., Edwards, G., Howard, D., Powell, J., Keywood, M., and Wang, F.:
1572 Comparison of mercury concentrations measured at several sites in the Southern Hemisphere,
1573 *Atmospheric Chemistry and Physics*, 15, 3125-3133, 2015.

1574 Sprovieri, F., Pirrone, N., Ebinghaus, R., Kock, H., and Dommergue, A.: A review of worldwide
1575 atmospheric mercury measurements, *Atmospheric Chemistry and Physics*, 10, 8245-8265, 2010.

1576 Streets, D. G., Devane, M. K., Lu, Z., Bond, T. C., Sunderland, E. M., and Jacob, D. J.: All-Time
1577 releases of mercury to the atmosphere from human activities, *Environmental Science & Technology*,
1578 45, 10485-10491, 2011.

1579 Sprovieri, F., Pirrone, N., Bencardino, M., amp, apos, Amore, F., Carbone, F., Cinnirella, S.,
1580 Mannarino, V., Landis, M., Ebinghaus, R., Weigelt, A., Brunke, E.-G., Labuschagne, C., Martin, L.,
1581 Munthe, J., W ängberg, I., Artaxo, P., Morais, F., Barbosa, H. d. M. J., Brito, J., Cairns, W., Barbante,
1582 C., Di éguéz, M. d. C., Garcia, P. E., Dommergue, A., Angot, H., Magand, O., Skov, H., Horvat, M.,
1583 Kotnik, J., Read, K. A., Neves, L. M., Gawlik, B. M., Sena, F., Mashyanov, N., Obolkin, V., Wip,
1584 D., Feng, X. B., Zhang, H., Fu, X., Ramachandran, R., Cossa, D., Knoery, J., Maruszczak, N.,
1585 Nerentorp, M., and Norstrom, C.: Atmospheric mercury concentrations observed at ground-based
1586 monitoring sites globally distributed in the framework of the GMOS network, *Atmospheric
1587 Chemistry and Physics*, 16, 11915-11935, 2016.

1588 Sprovieri, F., Pirrone, N., Bencardino, M., amp, apos, Amore, F., Angot, H., Barbante, C., Brunke,

1589 E.-G., Arcega-Cabrera, F., Cairns, W., Comero, S., Di éguez, M. d. C., Dommergue, A., Ebinghaus,
1590 R., Feng, X. B., Fu, X., Garcia, P. E., Gawlik, B. M., Hageström, U., Hansson, K., Horvat, M.,
1591 Kotnik, J., Labuschagne, C., Magand, O., Martin, L., Mashyanov, N., Mkololo, T., Munthe, J.,
1592 Obolkin, V., Ramirez Islas, M., Sena, F., Somerset, V., Spandow, P., Vardè M., Walters, C.,
1593 W ängberg, I., Weigelt, A., Yang, X., and Zhang, H.: Five-year records of mercury wet deposition
1594 flux at GMOS sites in the Northern and Southern hemispheres, *Atmospheric Chemistry and Physics*,
1595 17, 2689-2708, 2017

1596 Steffen, A., Scherz, T., Olson, M., Gay, D., and Blanchard, P.: A comparison of data quality control
1597 protocols for atmospheric mercury speciation measurements, *J Environ Monit*, 14, 752-765, 2012.

1598 Sung, J.-H., Roy, D., Oh, J.-S., Back, S.-K., Jang, H.-N., Kim, S.-H., Seo, Y.-C., Kim, J.-H., Lee, C.
1599 B., and Han, Y.-J.: Trans-boundary movement of mercury in the Northeast Asian region predicted
1600 by CAMQ-Hg from anthropogenic emissions distribution, *Atmospheric Research*, 203, 197-206,
1601 2018.

1602 Arctic Monitoring and Assessment Programme and United Nations Environment Programme
1603 (AMAP/UNEP): Global Hg assessment 2013: sources, emissions, releases and environmental
1604 transport, AMAP/UNEP, Geneva, Switzerland, 2013

1605 Arctic Monitoring and Assessment Programme and United Nations Environment Programme
1606 (AMAP/UNEP): Global mercury assessment 2018 - draft technical background document,
1607 AMAP/UNEP, Geneva, Switzerland, 2018.

1608 Wang, X., Lin, C.-J., Yuan, W., Sommar, J., Zhu, W., and Feng, X.: Emission-dominated gas
1609 exchange of elemental mercury vapor over natural surfaces in China, *Atmospheric Chemistry and*
1610 *Physics*, 16, 11125-11143, 2016.

1611 Wang, Y. Q., Zhang, X. Y., and Draxler, R. R.: TrajStat: GIS-based software that uses various
1612 trajectory statistical analysis methods to identify potential sources from long-term air pollution
1613 measurement data, Elsevier Science Publishers B. V., 938-939 pp., 2009.

1614 Weigelt, A., Ebinghaus, R., Manning, A. J., Derwent, R. G., Simmonds, P. G., Spain, T. G., Jennings,
1615 S. G., and Slemr, F.: Analysis and interpretation of 18 years of mercury observations since 1996 at
1616 Mace Head, Ireland, *Atmospheric Environment*, 100, 85-93, 2015.

1617 Wu, Q., Wang, S., Li, G., Liang, S., Lin, C. J., Wang, Y., Cai, S., Liu, K., and Hao, J.: Temporal
1618 trend and spatial distribution of speciated atmospheric mercury emissions in China during 1978-

1619 2014, *Environmental Science & Technology*, 50, 13428-13435, 2016.

1620 Xu, X., and Akhtar, U. S.: Identification of potential regional sources of atmospheric total gaseous
1621 mercury in Windsor, Ontario, Canada using hybrid receptor modeling, *Atmospheric Chemistry and*
1622 *Physics*, 10, 7073-7083, 2010.

1623 Yu Q, Luo Y, Wang S, Wang Z, Hao J, Duan L. Gaseous Elemental Mercury (GEM) Fluxes over
1624 Canopy of Two Typical Subtropical Forests in South China. *Atmospheric Chemistry and Physics*,
1625 18(1), 495-509, 2018.

1626 Zhang, G. Y., Zhou, L. M., Zheng, X. M., and Huang, W. D.: Temporal distribution and potential
1627 hazards of wet deposition mercury in Yangtze River Estuary, *Urban Environmental & Urban Ecology*,
1628 1-4, 2010.

1629 Zhang, H., Fu, X. W., Lin, C. J., Wang, X., and Feng, X. B.: Observation and analysis of speciated
1630 atmospheric mercury in Shangri-La, Tibetan Plateau, China, *Atmospheric Chemistry and Physics*,
1631 15, 653-665, 2015.

1632 Zhang, H., Fu, X. W., Lin, C.-J., Shang, L. H., Zhang, Y. P., Feng, X. B., and Lin, C.: Monsoon-
1633 facilitated characteristics and transport of atmospheric mercury at a high-altitude background site
1634 in southwestern China, *Atmospheric Chemistry and Physics*, 16, 13131-13148, 2016.

1635 Zhang, L., Wang, S. X., Wang, L., Wu, Y., Duan, L., Wu, Q. R., Wang, F. Y., Yang, M., Yang, H.,
1636 Hao, J. M., and Liu, X.: Updated emission inventories for speciated atmospheric mercury from
1637 anthropogenic sources in China, *Environmental Science & Technology*, 49, 3185-3194, 2015.

1638 Zhang, L. M., Wright, L. P., and Blanchard, P.: A review of current knowledge concerning dry
1639 deposition of atmospheric mercury, *Atmospheric Environment*, 43, 5853-5864, 2009.

1640 Zhang, Y. X., Jacob, D. J., Horowitz, H. M., Chen, L., Amos, H. M., Krabbenhoft, D. P., Slemr, F.,
1641 St Louis, V. L., and Sunderland, E. M.: Observed decrease in atmospheric mercury explained by
1642 global decline in anthropogenic emissions, *Proceedings of the National Academy of Sciences of the*
1643 *United States of America*, 113, 526, 2016.

1644 Zhao, B., Wang, S. X., Liu, H., Xu, J. Y., Fu, K., Klimont, Z., Hao, J. M., He, K. B., Cofala, J., and
1645 Amann, M.: NO_x emissions in China: historical trends and future perspectives, *Atmospheric*
1646 *Chemistry and Physics*, 13, 9869-9897, 2013.

1647 Zhu, J., Wang, T., Talbot, R., Mao, H., Hall, C. B., Yang, X., Fu, C., Zhuang, B., Li, S., Han, Y., and
1648 Huang, X.: Characteristics of atmospheric total gaseous mercury (TGM) observed in urban Nanjing,

1649 China, Atmospheric Chemistry and Physics, 12, 12103-12118, 2012.

1650

Figure citation

Figure 1. The location of the Chongming monitoring site in Shanghai, China

Figure 2. Monthly average GEM concentrations during the studied period (a) observed monthly GEM concentrations (b) GEM trend after decomposition (c) GEM seasonality after decomposition (d) GEM random after decomposition

Note: The observed concentrations during July 2015-April 2016 were TGM concentrations indeed due to the problems of Tekran 1130/1135. However, the GOM concentrations at Chongming Island accounted for less than 1% of TGM. Thus, the GEM concentrations were approximated to TGM concentrations during July 2015-April 2016.

Figure 3. Monthly variations of GEM concentration at remote sites in China

Figure 4. Seasonal cycle of GEM concentrations and emissions during 2014-2016. The error bars represent the standard deviation of seasonal average. Negative values of natural emissions represent mercury deposition and positive values of natural emissions represent natural emissions.

Figure 5. Source regions of GEM at monitoring site from PSCF model in 2014(a) and 2016(b)

Figure 6. The back trajectories map for cluster NCP, SW-YRD and ABROAD in 2014(a) and 2016(b)

(NCP – North China Plain; SW-YRD –Southwest region and Yangtze River Delta; ABROAD – Abroad)

Table citation

Table 1. PCA component loading of GEM and the co-pollutants

Table 2. Main air pollutant emitted by the different sector in YRD region in 2014

Table 3. The statistics of cluster and estimated contribution of GEM reduction in 2014 and 2016

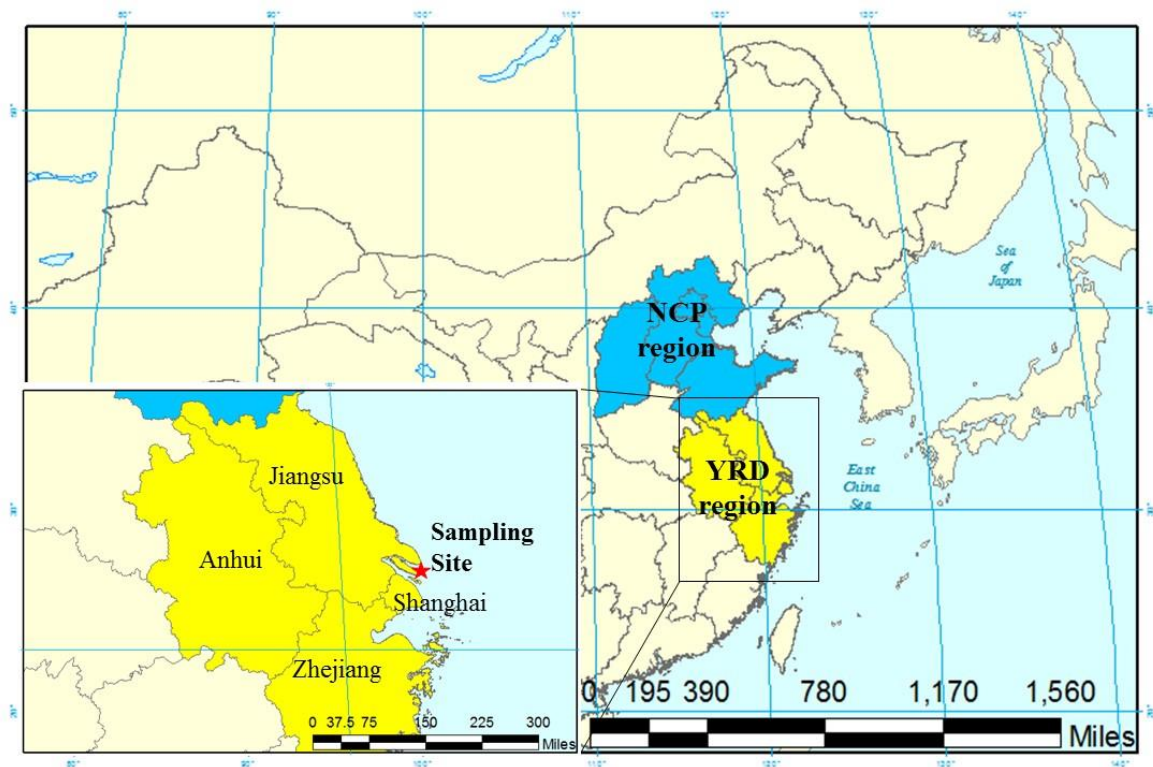


Figure 1. The location of the Chongming monitoring site in Shanghai, China

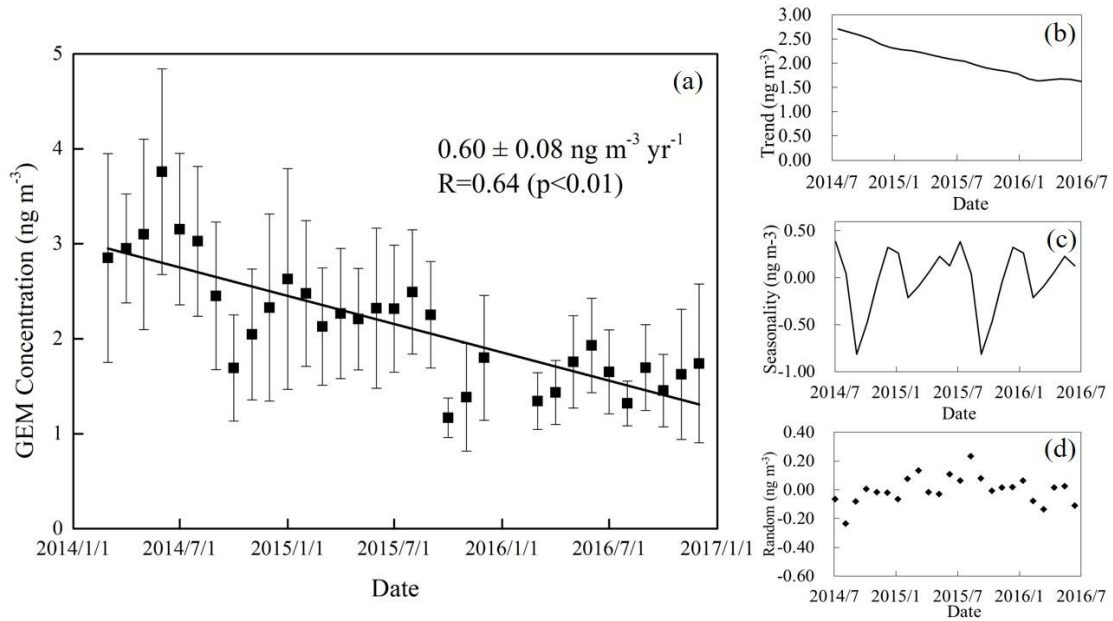


Figure 2. Monthly average GEM concentrations during the studied period (a) observed monthly GEM concentrations (b) GEM trend after decomposition (c) GEM seasonality after decomposition (d) GEM random after decomposition

Note: The observed concentrations during July 2015-April 2016 were TGM concentrations indeed due to the problems of Tekran 1130/1135. However, the GOM concentrations at Chongming Island accounted for less than 1% of TGM. Thus, the GEM concentrations were approximated to TGM concentrations during July 2015-April 2016.

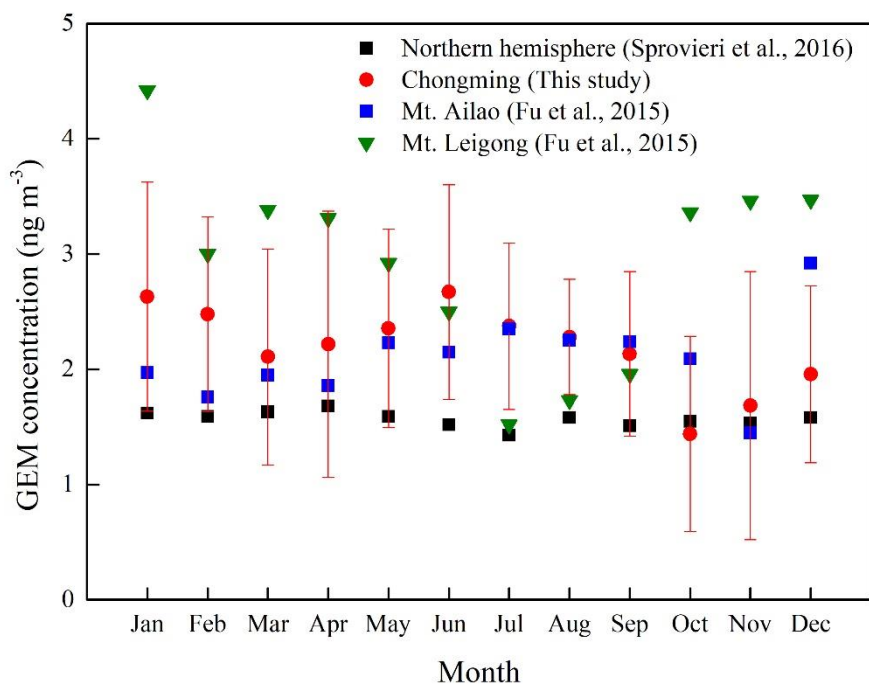


Figure 3. Monthly variations of GEM concentration at remote sites in China

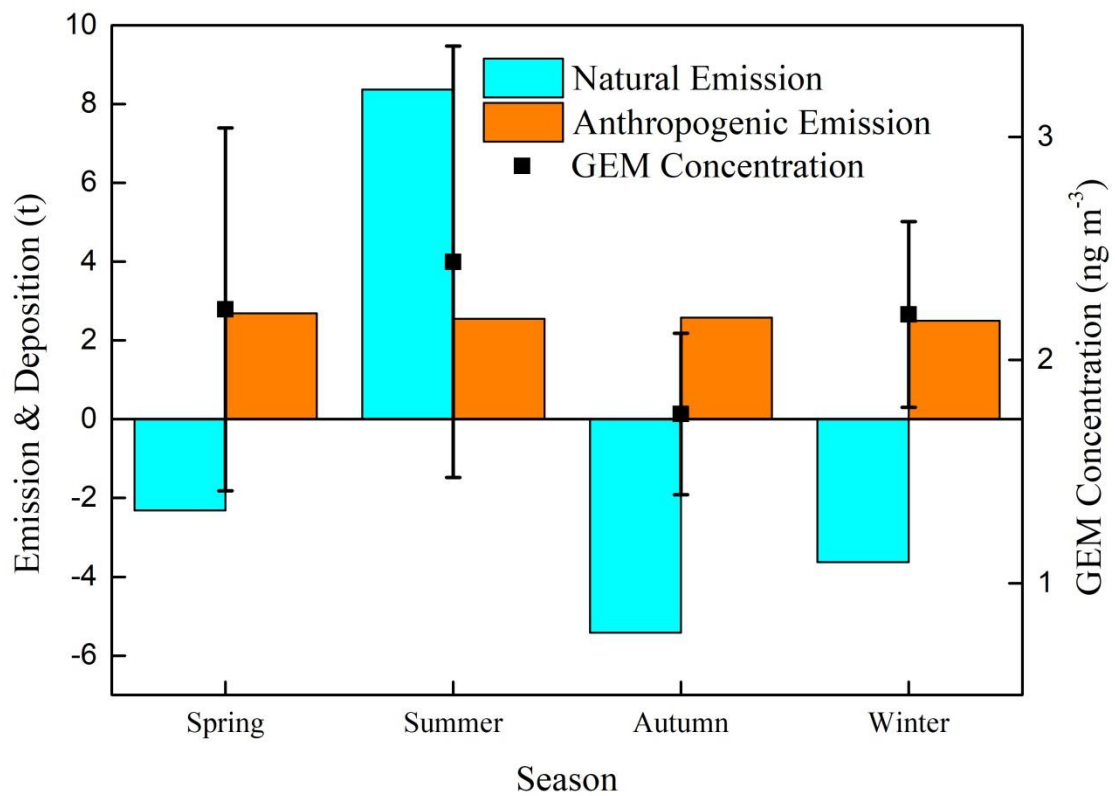
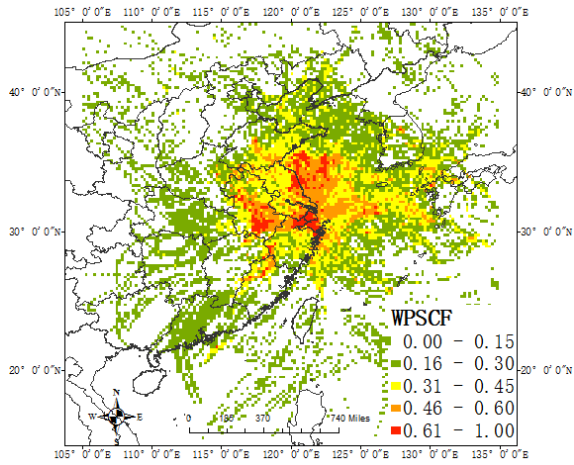
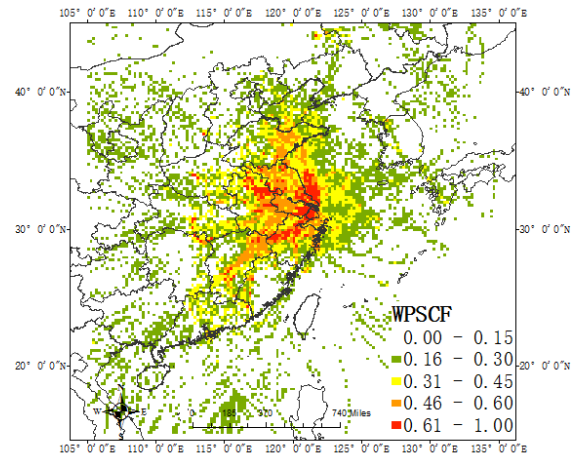


Figure 4. Seasonal cycle of GEM concentrations and natural emissions during 2014-2016. The error bars represent the standard deviation of seasonal average. Positive values of natural emissions represent Hg emitted to air. Otherwise, negative values represent Hg deposition.

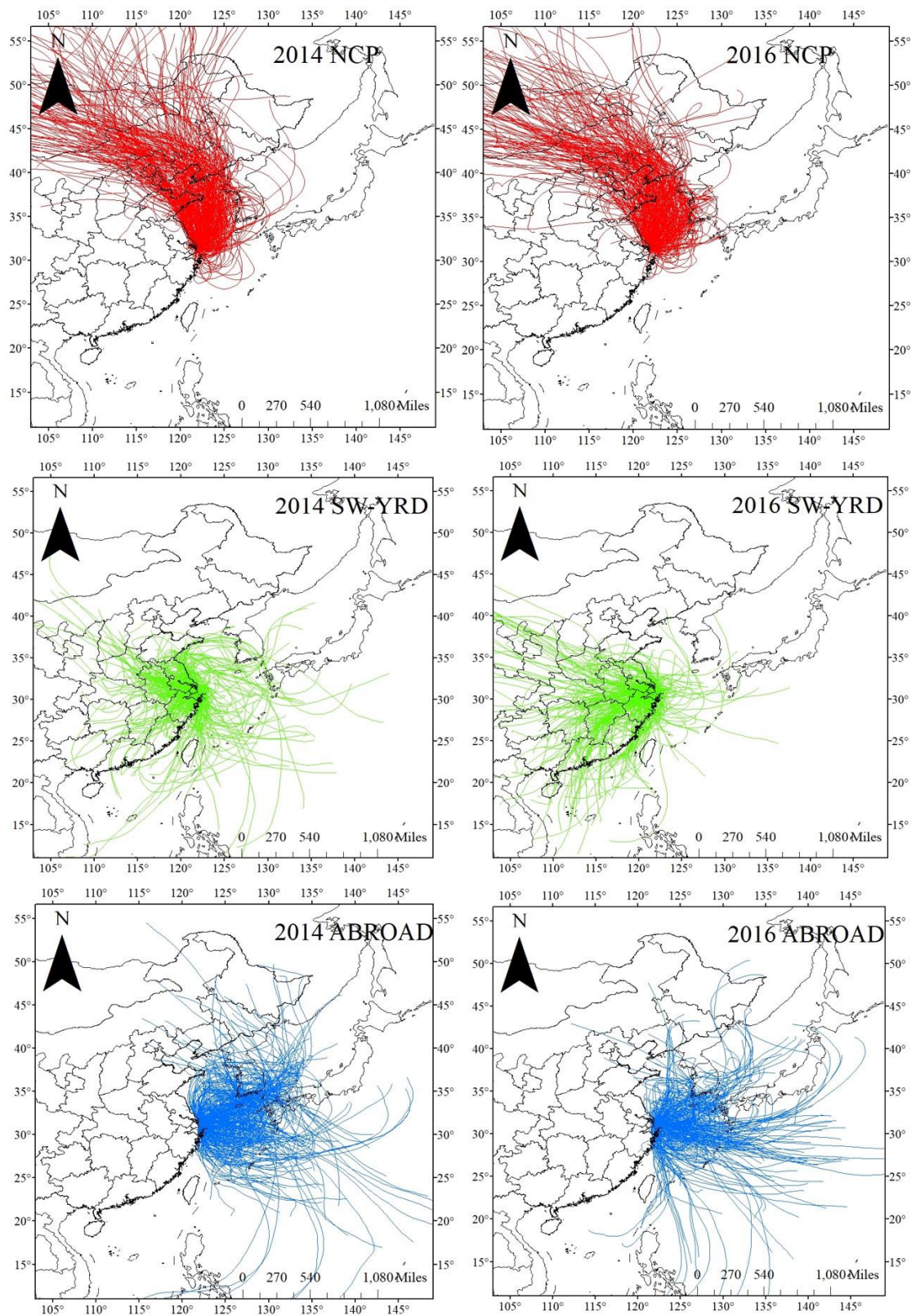


(a) 2014



(b) 2016

Figure 5. Source regions of GEM at monitoring site from PSCF model in 2014(a) and 2016(b)



(a) 2014

(b) 2016

Figure 6. The back trajectories map for cluster NCP, SW-YRD and ABROAD in 2014(a) and 2016(b)

(NCP – North China Plain; SW-YRD –Southwest region and Yangtze River Delta; ABROAD –
Abroad)

Table 1. PCA component loading of GEM and other air pollutants

Air pollutants	2014		Air pollutants	2016	
	Factor 1	Factor 2		Factor 1	Factor 2
SO ₂	0.76	0.14	SO ₂	0.82	-0.09
NO _x	0.76	-0.20	NO _x	0.70	-0.52
O ₃	-0.11	0.98	O ₃	-0.41	0.97
PM _{2.5}	0.85	0.05	PM _{2.5}	0.88	0.05
GEM	0.66	0.02	GEM	0.78	-0.19
CO	0.79	0.12			
Component	Combustion	Transport of air mass from stratosphere	Component	Combustion	Transport of air mass from stratosphere
Variance explain (%)	49.36	17.53	Variance explain (%)	50.63	25.10

Note: Text in bold phase were regarded as high loading (factor loading > 0.40 or < -0.40)

Table 2. Emissions of the main air pollutants in YRD region in 2014

Emission sectors	Annual emissions			
	SO ₂ (kt)	NO _x (kt)	PM _{2.5} (kt)	GEM (t)
Coal-fired power plants	918.31	991.62	118.42	14.00
Coal-fired industrial boilers	311.03	271.94	79.91	9.80
Residential coal combustion	68.48	42.11	163.93	0.40
Cement clinker production	207.48	371.13	208.02	4.70
Iron and steel production	480.97	142.80	169.84	2.30
Mobile oil combustion	38.43	1786.74	98.00	1.90
Other sectors	348.83	316.28	382.48	2.50

Table 3. The statistics of cluster and estimated contribution of GEM reduction in 2014 and 2016

Time	Cluster	Trajectories			GEM concentration, C_j (ng m ⁻³)	Trajectory weighted concentration, TWC_j (ng m ⁻³)	Contribution to GEM reduction, CR_i
		Numbers	Ratio	Average Ratio (AR)			
2014	NCP	285	33%	32%	2.33	0.79	
	SW-YRD	304	35%	37%	3.19	1.18	
	ABROAD	275	32%	31%	2.58	0.77	
2016	NCP	237	31%	32%	1.48	0.50	26%
	SW-YRD	302	39%	37%	1.87	0.69	44%
	ABROAD	230	30%	31%	1.44	0.43	30%

Supporting information for “Recent decrease trend of atmospheric mercury concentrations in East China: the influence of anthropogenic emissions ”

Yi Tang^{1,2}, Shuxiao Wang^{1,2*}, Qingru Wu^{1,2*}, Kaiyun Liu^{1,2}, Long Wang³, Shu Li¹, Wei Gao⁴, Lei Zhang⁵, Haotian Zheng^{1,2}, Zhijian Li¹, Jiming Hao^{1,2}

¹ State Key Joint Laboratory of Environmental Simulation and Pollution Control, School of Environment, Tsinghua University, Beijing 100084, China

² State Environmental Protection Key Laboratory of Sources and Control of Air Pollution Complex, Beijing 100084, China

³ School of Environment and Energy, South China University of Technology, Guangzhou, 510006, China

⁴ Yangtze River Delta Center for Environmental Meteorology Prediction and Warning, Shanghai, 20030, China

⁵ State Key Laboratory of Pollution Control & Resource Reuse, School of the Environment, Nanjing University, Nanjing, 210023, China

12 pages (including cover page)

4 Figures (S1, S2, S3, S4)

6 Tables (S1, S2, S3, S4, S5, S6)

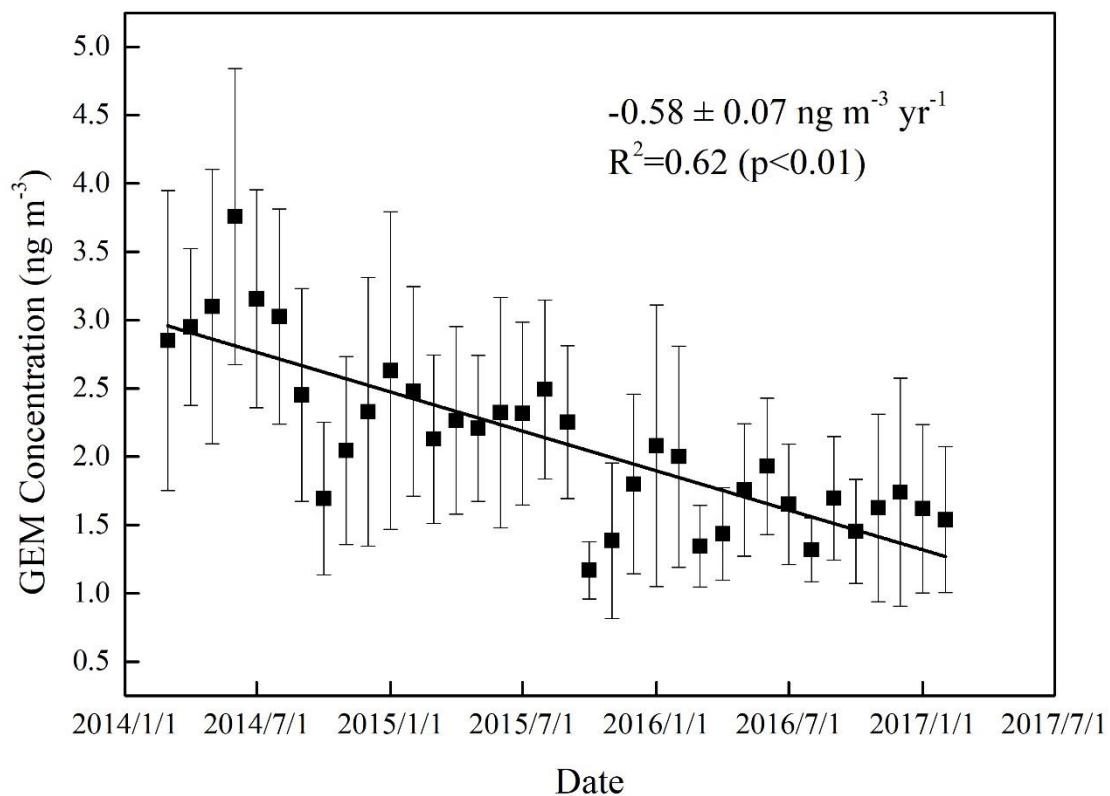


Figure S1. The trend of monthly average GEM concentration from March 2014 to February 2017. The monthly average of GEM in January of 2016 is simulated as the average value that in the January of 2015 and 2017. The same method is used for the data in February of 2016.

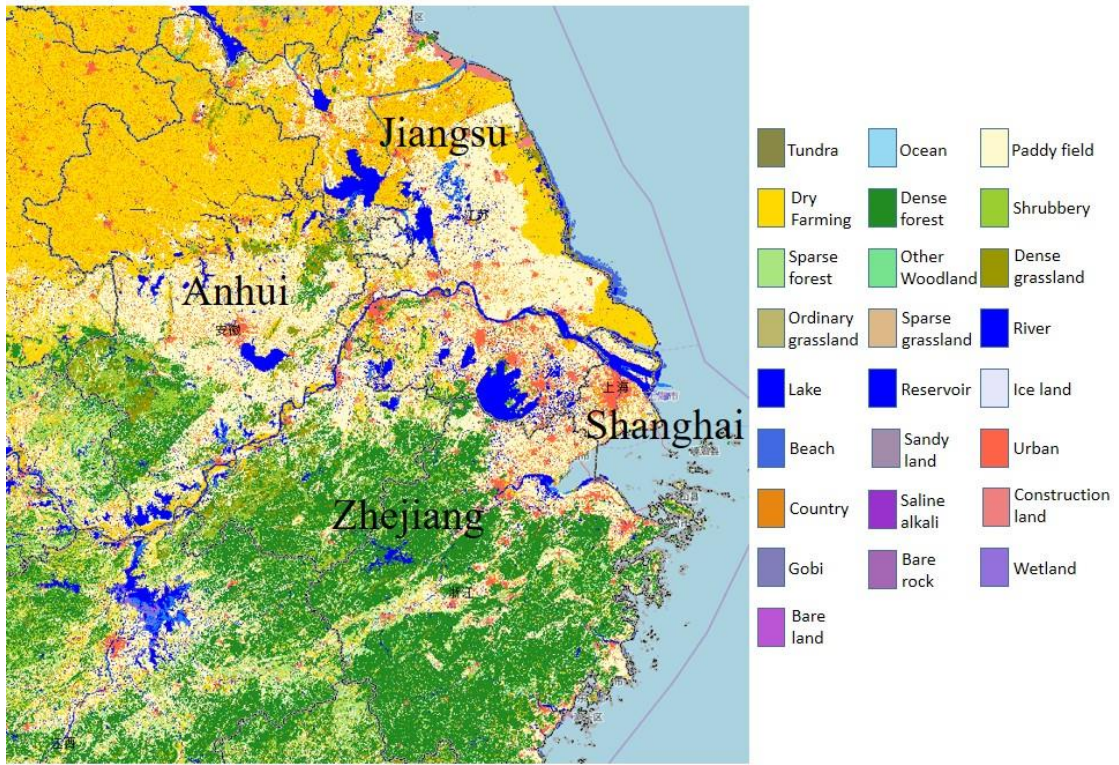


Figure S2. Land use type of YRD region in 2015

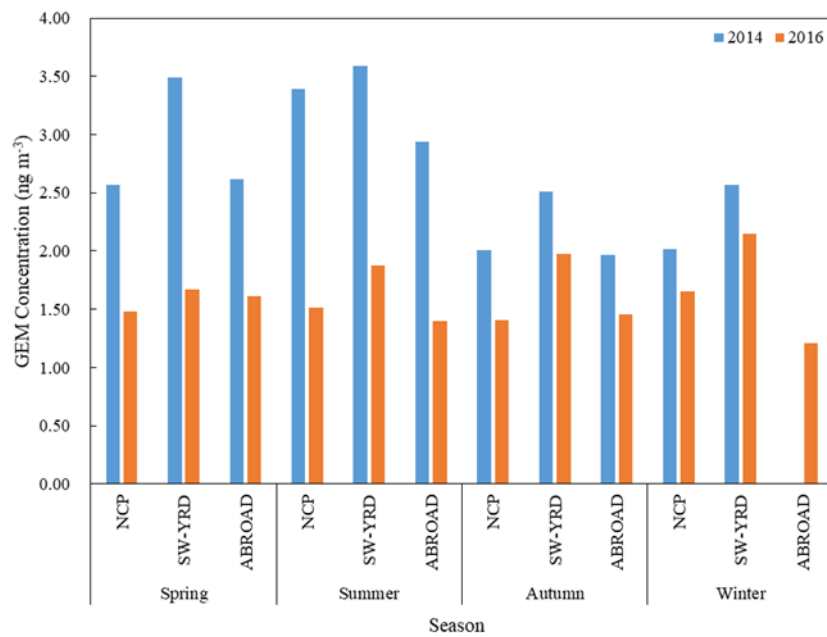


Figure S3. The seasonality of GEM concentration in the NCP, SW-YRD and ABROAD region (No trajectory transport though ABROAD in winter of 2014)

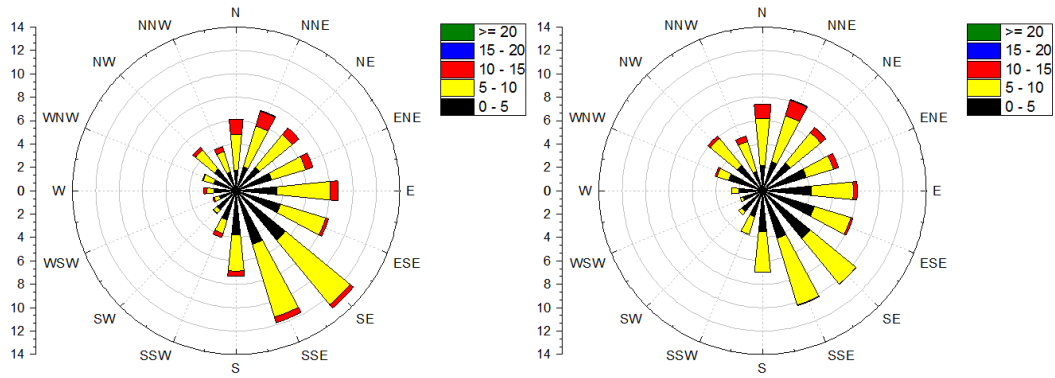


Figure S4. Wind rose at Chongming island in 2014 and 2016

Table S1. Monthly distribution factor for cement clinker production, coal-fired power plants, coal-fired industrial boilers, resident coal combustion, cement clinker production, iron and steel production in potential sources region in 2014 and 2016

Cement clinker production									
2014	Shanghai	Jiangsu	Zhejiang	Anhui	2016	Shanghai	Jiangsu	Zhejiang	Anhui
Jan	0.10	0.06	0.10	0.10	Jan	0.00	0.00	0.00	0.00
Feb	0.00	0.00	0.00	0.00	Feb	0.00	0.00	0.00	0.00
Mar	0.08	0.09	0.08	0.09	Mar	0.04	0.13	0.11	0.11
Apr	0.09	0.09	0.10	0.09	Apr	0.22	0.14	0.10	0.05
May	0.09	0.10	0.09	0.10	May	0.08	0.11	0.10	0.07
Jun	0.09	0.09	0.08	0.09	Jun	0.08	0.13	0.09	0.07
Jul	0.09	0.09	0.08	0.09	Jul	0.09	0.11	0.10	0.07
Aug	0.09	0.09	0.08	0.09	Aug	0.06	0.10	0.08	0.07
Sep	0.08	0.10	0.09	0.08	Sep	0.11	0.09	0.08	0.10
Oct	0.10	0.10	0.10	0.09	Oct	0.08	0.08	0.10	0.09
Nov	0.10	0.10	0.10	0.10	Nov	0.13	0.05	0.11	0.17
Dec	0.10	0.10	0.10	0.10	Dec	0.12	0.06	0.12	0.20
Coal-fired power plants									
2014	Shanghai	Jiangsu	Zhejiang	Anhui	2016	Shanghai	Jiangsu	Zhejiang	Anhui
Jan	0.10	0.08	0.07	0.09	Jan	0.10	0.08	0.07	0.09
Feb	0.10	0.07	0.07	0.08	Feb	0.09	0.07	0.07	0.08
Mar	0.11	0.09	0.09	0.09	Mar	0.09	0.09	0.10	0.08
Apr	0.09	0.10	0.09	0.08	Apr	0.07	0.08	0.08	0.08
May	0.09	0.09	0.09	0.08	May	0.07	0.08	0.08	0.07
Jun	0.07	0.08	0.08	0.08	Jun	0.06	0.08	0.08	0.07
Jul	0.08	0.09	0.09	0.10	Jul	0.10	0.09	0.10	0.09
Aug	0.07	0.08	0.08	0.09	Aug	0.11	0.10	0.10	0.10
Sep	0.05	0.07	0.07	0.07	Sep	0.07	0.08	0.08	0.08
Oct	0.05	0.08	0.08	0.07	Oct	0.07	0.08	0.08	0.07
Nov	0.07	0.08	0.09	0.08	Nov	0.07	0.08	0.08	0.08
Dec	0.11	0.10	0.10	0.09	Dec	0.10	0.09	0.10	0.10
Iron and steel production									
2014	Shanghai	Jiangsu	Zhejiang	Anhui	2016	Shanghai	Jiangsu	Zhejiang	Anhui
Jan	0.09	0.08	0.07	0.07	Jan	0.09	0.08	0.07	0.07
Feb	0.08	0.07	0.07	0.07	Feb	0.09	0.08	0.07	0.07
Mar	0.09	0.08	0.09	0.08	Mar	0.09	0.09	0.09	0.08
Apr	0.09	0.08	0.09	0.08	Apr	0.09	0.09	0.10	0.08
May	0.09	0.08	0.08	0.09	May	0.09	0.08	0.09	0.08
Jun	0.09	0.08	0.09	0.09	Jun	0.08	0.09	0.09	0.08
Jul	0.09	0.08	0.08	0.09	Jul	0.08	0.08	0.09	0.08
Aug	0.09	0.07	0.08	0.09	Aug	0.08	0.08	0.08	0.13
Sep	0.07	0.08	0.08	0.09	Sep	0.08	0.08	0.08	0.08
Oct	0.07	0.08	0.08	0.09	Oct	0.08	0.08	0.08	0.09

Nov	0.07	0.08	0.09	0.08	Nov	0.08	0.08	0.08	0.09
Dec	0.09	0.13	0.10	0.08	Dec	0.08	0.08	0.09	0.09
Coal-fired industrial boilers									
2014	Shanghai	Jiangsu	Zhejiang	Anhui	2016	Shanghai	Jiangsu	Zhejiang	Anhui
Jan	0.09	0.08	0.08	0.09	Jan	0.08	0.07	0.08	0.08
Feb	0.08	0.08	0.07	0.09	Feb	0.08	0.07	0.08	0.07
Mar	0.07	0.09	0.09	0.10	Mar	0.09	0.08	0.09	0.09
Apr	0.06	0.08	0.09	0.09	Apr	0.08	0.08	0.09	0.09
May	0.09	0.09	0.08	0.08	May	0.09	0.09	0.08	0.08
Jun	0.09	0.09	0.07	0.08	Jun	0.08	0.08	0.08	0.08
Jul	0.09	0.08	0.08	0.07	Jul	0.08	0.08	0.09	0.09
Aug	0.09	0.07	0.08	0.08	Aug	0.08	0.08	0.08	0.08
Sep	0.08	0.09	0.08	0.09	Sep	0.08	0.08	0.08	0.08
Oct	0.08	0.08	0.09	0.08	Oct	0.09	0.09	0.09	0.09
Nov	0.08	0.08	0.09	0.07	Nov	0.08	0.09	0.09	0.08
Dec	0.09	0.08	0.09	0.08	Dec	0.09	0.09	0.09	0.08
Residential coal combustion									
2014	Shanghai	Jiangsu	Zhejiang	Anhui	2016	Shanghai	Jiangsu	Zhejiang	Anhui
Jan	0.33	0.33	0.33	0.33	Jan	0.33	0.33	0.33	0.33
Feb	0.33	0.33	0.33	0.33	Feb	0.33	0.33	0.33	0.33
Mar	0.05	0.05	0.05	0.05	Mar	0.05	0.05	0.05	0.05
Apr	0.00	0.00	0.00	0.00	Apr	0.00	0.00	0.00	0.00
May	0.00	0.00	0.00	0.00	May	0.00	0.00	0.00	0.00
Jun	0.00	0.00	0.00	0.00	Jun	0.00	0.00	0.00	0.00
Jul	0.00	0.00	0.00	0.00	Jul	0.00	0.00	0.00	0.00
Aug	0.00	0.00	0.00	0.00	Aug	0.00	0.00	0.00	0.00
Sep	0.00	0.00	0.00	0.00	Sep	0.00	0.00	0.00	0.00
Oct	0.00	0.00	0.00	0.00	Oct	0.00	0.00	0.00	0.00
Nov	0.05	0.05	0.05	0.05	Nov	0.05	0.05	0.05	0.05
Dec	0.23	0.23	0.23	0.23	Dec	0.23	0.23	0.23	0.23

Table S2. The meteorological condition between 2014 and 2016 in Chongming

Month	Temperature		Solar Radiation		Relative Humidity	
	2014(°C)	2016(°C)	2014(W m ⁻²)	2016(W m ⁻²)	2014 (%)	2016 (%)
1		4.39		104.47		71.28
2		5.73		143.68		67.69
3	10.14	9.55	156.61	150.31	79.66	71.43
4	14.85	14.77	163.29	161.88	75.11	80.35
5	20.59	19.24	181.49	176.04	78.15	78.50
6	22.87	22.98	171.20	156.63	82.98	83.00
7	26.86	27.82	244.30	224.52	84.62	82.24
8	24.64	28.31	262.20	253.61	78.38	74.03
9	22.08	24.49	197.20	153.34	74.36	75.27
10	17.76	20.82	168.21	122.81	70.47	75.67
11	10.94	13.64	117.01	113.00	68.96	75.25
12	5.34	8.99	114.60	103.87	59.47	71.62
Average	17.61	16.73	177.61	155.35	75.22	75.53

Table S3. The amount of valid data during sampling period

Year	Jan	Feb	Mar	Apr	May	Jun	Jul	Aug	Sep	Oct	Nov	Dec
2014			5914	6125	6493	5568	4634	6255	6491	7106	7578	5564
2015	5227	4532	5216	3392	4072	4797	7591	6538	3434	2223	4363	8833
2016			1370	8293	7476	5884	5424	5641	3561	4544	6292	4589

Table S4. Historical variation trends of atmospheric Hg in previous studies

Monitoring site	Duration	TGM trend (pg m ⁻³ yr ⁻¹)	Variation trend	Site description	Monitoring instrument	References
Alert, Canada	2000-2009	-13(-21,0)	-0.9% y ⁻¹	Remote	2537A	Cole et al. 2013
Kuujuarapik, Canada	2000-2009	-33(-50,-18)	-2.1% y ⁻¹	Remote	2537A	Cole et al. 2013
Egbert, Canada	2000-2009	-35(-44,-27)	-2.2% y ⁻¹	Remote	2537A	Cole et al. 2013
Zeppelin Stn, Norway	2000-2009	+2(-7,+12)	no trend	Remote	2537A	Cole et al. 2013
St.Anicet, Canada	2000-2009	-29(-31,-27)	-1.9% y ⁻¹	Remote	2537A	Cole et al. 2013
Kejimkujik, Canada	2000-2009	-23(-33,-13)	-1.6% y ⁻¹	Remote	2537A	Cole et al. 2013
Head, Ireland	1996-2009		-1.3±0.2% y ⁻¹	Rural	2537A	Weigelt et al. 2015
Yong San, South Korea	2004-2011	No trend (3.54±1.46 ng m ³)		Urban	AM-3	Kim et al. 2016
Yong San, South Korea	2013-2014	Decrease to 2.34±0.73 ng m ³			AM-3	Kim et al. 2016
Mt. Changbai	2013-2015	Decrease from 1.74 ng m ⁻³ to 1.58 ng m ⁻³		Remote	2537B	Fu et al. 2015
Chongming Island, China	2014-2016	-600	-29.4%/y	Remote	2537X	This study

Table S5. The annual concentration of SO₂, NO_x, O₃ and PM_{2.5} at Chongming site, NCP, and SW-YRD regions

Year	2014			2016			Change			
Pollutants	Region	NCP	SW-YRD	Chongming	NCP	SW-YRD	Chongming	NCP	SW-YRD	Chongming
PM _{2.5} (µg m ⁻³)		71.93	53.05	25.09	60.75	44.75	23.89	-16%	-16%	-5%
SO ₂ (µg m ⁻³)		34.52	21.01	1.60	24.37	16.40	1.47	-29%	-22%	-8%
NO ₂ (µg m ⁻³)		45.07	34.34	12.62	41.55	34.40	10.84	-8%	0%	-14%
O ₃ (µg m ⁻³)		60.29	56.27	41.70	61.84	60.92	44.38	3%	8%	6%
GEM (ng m ⁻³)		No data		2.68	No data		1.60	No data		-40%

Note: According to the contribution of trajectory, the dominant provinces in the NCP region included Beijing, Tianjin, Hebei, Shandong and Liaoning province. The SW-YRD mainly contained Shanghai, Zhejiang, Jiangsu, Jiangxi and Anhui province.

Table S6. Emission inventories of the main pollutants from the studied regions in 2014 and 2016

Air pollutants	2014		2016		Decline proportion	
	NCP	SW-YRD	NCP	SW-YRD	NCP	SW-YRD
PM _{2.5} (kt)	2019	1209	1849	1109	-8%	-8%
NO _x (kt)	5697	4022	5424	3855	-5%	-4%
SO ₂ (kt)	3780	1993	3450	1780	-9%	-11%
GEM (t)	118	72	103	67	-13%	-7%

Note: According to the contribution of trajectory, the dominant provinces in the NCP region included Beijing, Tianjin, Hebei, Shandong and Liaoning province. The SW-YRD mainly contained Shanghai, Zhejiang, Jiangsu, Jiangxi and A